Published for SISSA by Springer

Received: March 12, 2020
Accepted: June 15, 2020
Published: July 13, 2020

Threshold factorization of the Drell-Yan process at next-to-leading power

Martin Beneke,[a] **Alessandro Broggio,**[b,c] **Sebastian Jaskiewicz**[a] **and Leonardo Vernazza**[d]

[a] *Physik Department T31, Technische Universität München, James-Franck-Straße 1, D–85748 Garching, Germany*
[b] *Università degli Studi di Milano-Bicocca, Piazza della Scienza 3, I–20126 Milano, Italy*
[c] *INFN, Sezione di Milano-Bicocca, Piazza della Scienza 3, I–20126 Milano, Italy*
[d] *Dipartimento di Fisica Teorica, Università di Torino, and INFN, Sezione di Torino, Via P. Giuria 1, I-10125 Torino, Italy*

E-mail: alessandro.broggio@unimib.it, sebastian.jaskiewicz@tum.de, leonardo.vernazza@to.infn.it

Abstract: We present a factorization theorem valid near the kinematic threshold $z = Q^2/\hat{s} \to 1$ of the partonic Drell-Yan process $q\bar{q} \to \gamma^* + X$ for general subleading powers in the $(1-z)$ expansion. We then consider the specific case of next-to-leading power. We discuss the emergence of collinear functions, which are a key ingredient to factorization starting at next-to-leading power. We calculate the relevant collinear functions at $\mathcal{O}(\alpha_s)$ by employing an operator matching equation and we compare our results to the expansion-by-regions computation up to the next-to-next-to-leading order, finding agreement. Factorization holds only before the dimensional regulator is removed, due to a divergent convolution when the collinear and soft functions are first expanded around $d = 4$ before the convolution is performed. This demonstrates an issue for threshold resummation beyond the leading-logarithmic accuracy at next-to-leading power.

Keywords: Effective Field Theories, Perturbative QCD, Resummation

ArXiv ePrint: 1912.01585

Open Access, © The Authors.
Article funded by SCOAP[3].

https://doi.org/10.1007/JHEP07(2020)078

JHEP07(2020)078

Contents

1 Introduction **1**

2 Threshold dynamics and collinear functions **2**
- 2.1 Leading power and decoupling 3
- 2.2 Emergence of collinear functions 6
- 2.3 Collinear matching: formal definitions 8

3 Factorization near threshold **10**
- 3.1 Factorization at general subleading powers 10
- 3.2 Factorization at NLP 14
  - 3.2.1 NLP kinematic correction $\Delta^{\rm kin}_{\rm NLP}(z)$ 17
  - 3.2.2 Dynamical NLP power correction $\Delta^{\rm dyn}_{\rm NLP}(z)$ 18
- 3.3 Expansion up to NNLO 20

4 Calculation of collinear functions **22**
- 4.1 Collinear functions at $\mathcal{O}(\alpha_s^0)$ 23
  - 4.1.1 Single soft gluon structures 23
  - 4.1.2 Double soft parton structures 26
- 4.2 Collinear functions at $\mathcal{O}(\alpha_s)$ 28
  - 4.2.1 Detailed computation 28
  - 4.2.2 Amplitude calculation results 30
  - 4.2.3 Collinear functions results at the one-loop order 31
  - 4.2.4 Relation to the LBK ampltiude and the radiative jet function 31

5 Fixed-order results **32**
- 5.1 NLO 33
- 5.2 NNLO 33
  - 5.2.1 Collinear contribution 34
  - 5.2.2 Hard contribution 34
  - 5.2.3 Soft contribution 35
  - 5.2.4 Kinematic contribution 36

6 Ill-defined convolution **36**

7 Summary **38**

A Subleading SCET Lagrangian **39**
- A.1 Quark-gluon subleading SCET Lagrangian 39
- A.2 YM subleading SCET Lagrangian 40

JHEP07(2020)078

B One-loop single soft real emission amplitude **41**
B.1 Collinear loop: $\gamma_{\perp\rho}$ 42
B.2 Collinear loop: n_-^ρ and n_+^ρ 43
B.3 Soft loop: $\gamma_{\perp\rho}$ 43
B.4 Soft loop: n_+^ρ 45
B.5 Hard loop: $\gamma_{\perp\rho}$ 46
B.6 Hard loop: n_+^ρ 46

1 Introduction

The study of soft emission in the threshold regime $z = Q^2/\hat{s} \to 1$ of the Drell-Yan (DY) process $A + B \to \gamma^*(Q) + X$ has a long history. The all-order summation of the leading-power (LP) logarithms in $(1 - z)$ was pioneered in [1, 2] and was later studied using soft-collinear effective theory (SCET) methods [3–5]. Currently LP threshold logarithms can be resummed up to next-to-next-to-next-to-leading logarithmic accuracy [5, 6]. In comparison, the structure of factorization and resummation at the next-to-leading power (NLP), that is, the next order in the expansion in $(1 - z)$, is not very well understood.

The DY process, given it is the simplest hadron-hadron collision process, has also been the target of several new calculations at subleading power. In this direction explicit computations of partonic cross sections at NLP up to next-to-next-to-leading order (NNLO) and partly beyond were performed in the coupling expansion by employing the expansion-by-regions method [7, 8] and diagrammatic factorization techniques [9–13]. The leading logarithmic (LL) resummation of the Drell-Yan processes $q\bar{q} \to \gamma^* + X$ and $gg \to H + X$ was first achieved using SCET methods [14, 15] and soon after in the diagrammatic framework [16]. Besides the threshold regime, the analysis of subleading power corrections for DY and single Higgs production has been investigated at fixed-order for resolution variables such as N-jettiness [17–22] and the q_T of the lepton pair or the Higgs boson [23, 24]. The resummation of NLP LLs for an event shape can be found in [25].

The resummation of NLP leading logarithms [14, 15] relies on a factorization formula that was anticipated in these papers, and is also a prerequisite for taking the non-trivial step beyond LLs. In the present work we fill the theoretical gaps and provide the details of the derivation of the factorization formula beyond LP for $q\bar{q} \to \gamma^* + X$. The factorization formula, which achieves the separation of scales through operator definitions of the relevant functions, and its check against the existing NNLO NLP results from the expansion-by-regions approach, is the first main result of this paper. Nevertheless, it must be regarded as a formal result, because it applies to bare regularized quantities. As will be explained, when one attempts to renormalize these quantities by subtracting the divergent parts, the convolution of the various factors becomes itself divergent. This complicates the resummation of NLP logarithms beyond the LL accuracy with SCET renormalization group methods.

JHEP07(2020)078

The second main result of this paper, already extensively used in [14, 15], is the identification of *collinear functions* or radiative jet functions at the amplitude level in the factorization formula at NLP. We discuss their origin, why they do not appear in the well-known LP factorization formula, and provide their precise operator definition in SCET. We also calculate the collinear functions at $\mathcal{O}(\alpha_s)$, which illustrates the concept at the practical level and is required for the above mentioned NNLO comparison.

The concept of a jet function radiating a soft gluon was originally introduced in [26] by way of extending the Low-Burnett-Kroll formula in QED. It has been extensively discussed in the diagrammatic factorization approach [12, 13, 27] for the production of a colourless final state in hadronic collisions. While these functions are closely related to the collinear functions above, since they describe the same physics, they are yet different. The collinear functions in SCET are defined at the operator level as the matrix elements of collinear fields. They are single scale objects, excluding soft contributions, and therefore appear suitable for the formulation of the NLP factorization formula.

The paper is structured as follows. In section 2 we discuss the emergence of the collinear functions and provide their definition through an operator matching equation. The factorization formula valid at general subleading powers is derived in section 3. We then specialize this formula to NLP and identify the relevant soft and collinear functions which appear at this order in the power expansion. We present one of the main results of our paper in section 4 where we extract the collinear functions at $\mathcal{O}(\alpha_s)$ through a matching calculation. We compare the result that we obtain for the factorized cross section, where we employ the newly computed collinear functions, to the expansion-by-regions results up to NNLO in fixed-order perturbation theory [12, 13] in section 5. In particular, we find agreement with the collinear-soft NNLO contribution, if the convolution of collinear and soft function is performed in d dimensions. In section 6 we demonstrate the appearance of a divergent convolution when we expand the collinear and soft function in $d-4$ before performing the convolution between the two. We conclude in section 7. The NLP SCET Lagrangian and supplementary results for the NLP one-loop soft emission amplitude are provided in appendices A and B, respectively.

2 Threshold dynamics and collinear functions

The object of our investigation is the partonic DY process $q\bar{q} \to \gamma^*[\to \ell\bar{\ell}] + X$ in the kinematic region $z = Q^2/\hat{s} \to 1$, where $\hat{s} = x_a x_b\, s$ is the partonic centre-of-mass energy squared, x_a, x_b are the momentum fractions of the partons inside the incoming hadrons and Q^2 is the invariant mass squared of the lepton pair. The factorization of the Drell-Yan process near threshold at NLP will be conducted within the position-space formulation [28, 29] of SCET [30, 31]. Four-momenta will often be decomposed using light-like vectors n_+^μ and n_-^μ satisfying $n_+ \cdot n_- = 2$ and $n_-^2 = n_+^2 = 0$, according to

$$p^\mu = (n_+ p)\frac{n_-^\mu}{2} + (n_- p)\frac{n_+^\mu}{2} + p_\perp^\mu \,. \tag{2.1}$$

At the partonic level, the threshold configuration constitutes a $\mathrm{SCET_I}$ problem, hence to capture the dynamics, collinear, anticollinear, and soft fields are required. The scaling of

JHEP07(2020)078

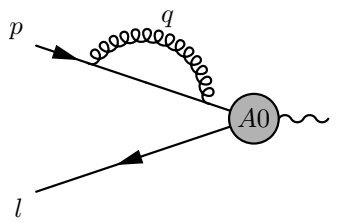

Figure 1. Example of a threshold-collinear loop attached to the external PDF-collinear line together with a LP (A0) current. This diagram, and the ones with more loops attaching to the (anti)collinear leg, yield scaleless integrals and therefore vanish in dimensional regularization.

the corresponding momenta, written in component notation $(n_+p, n_-p, p_\perp)$, is $Q(1, \lambda^2, \lambda)$, $Q(\lambda^2, 1, \lambda)$, and $Q(\lambda^2, \lambda^2, \lambda^2)$, respectively, where Q is the hard scale of the process and λ is the small power-counting parameter given by $\lambda = \sqrt{1-z}$. We note that threshold-collinear modes cannot be radiated into the final state X, since there is not enough energy available in threshold kinematics.

At the hadronic level, (anti)collinear-PDF modes with transverse momentum scaling $p_\perp \sim \Lambda$, where Λ denotes the strong interaction scale, exist in addition to the above threshold-collinear modes. These *can* be radiated into the hadronic final state. The ordinary parton distribution functions are defined in terms of these modes. Concretely, the c-PDF modes have momentum scaling $(Q, \Lambda^2/Q, \Lambda)$, whereas it is $(\Lambda^2/Q, Q, \Lambda)$ for the $\bar{c}$-PDF modes. We assume that the scale Λ of the strong interaction is parametrically much smaller than the threshold-collinear scale, $\Lambda \ll Q\lambda = Q(1-z)^{1/2}$. We consider power corrections in λ, but we always work at leading power in Λ/Q.

In the derivation of the LP factorization theorem the threshold-collinear fields are usually ignored, since they can be trivially integrated out. This can be traced to the soft-collinear decoupling transformation [31], which removes completely the soft-collinear interactions from the LP Lagrangian. As is well known, the LP partonic cross section is then factorized at threshold into the convolution of a hard function, which is the square of a hard matching coefficient, and a soft function, which is a vacuum matrix element of soft Wilson lines [32]. At subleading power, soft-collinear interactions remain after the decoupling transformation, resulting in time-ordered product operators [33]. Threshold-collinear loops no longer vanish, and the threshold-collinear fields must now be matched to c-PDF collinear fields. The non-trivial matching coefficients constitute the *amplitude-level collinear functions*. In the following we will make these qualitative statements more precise.

2.1 Leading power and decoupling

We begin the discussion by considering the purely threshold-collinear[1] loop corrections to the DY process, as depicted in figure 1. The LP current, denoted $J^{A0,A0}$ following the notation of [34], consists of a collinear quark field in the n_-^μ direction and an anticollinear antiquark field in the n_+^μ direction. The first important observation is that on-shell such loops yield scaleless integrals, which vanish in dimensional regularization.

[1]In the following, we will often refer to these as simply "collinear". "Purely collinear" means loops without soft attachments.

JHEP07(2020)078

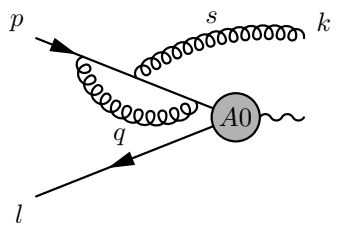

Figure 2. Example of a LP diagram with a collinear loop and a LP soft emission. This diagram is non-vanishing.

In order to obtain non-vanishing corrections, the introduction of an additional scale is necessary, for example, through the injection of a soft momentum. This is possible in threshold kinematics since the final state is composed of soft radiation. To this end, we consider the LP SCET Lagrangian written in terms of standard SCET fields,

$$\mathcal{L}^{(0)}(z) = \bar{\xi}_c \left(in_- D + i\not{D}_{c\perp} \frac{1}{in_+ D_c} i\not{D}_{c\perp} \right) \frac{\not{n}_+}{2} \xi_c + \mathcal{L}_s^{(0)}(z) + \mathcal{L}_{\rm YM}^{(0)}(z)\,, \tag{2.2}$$

where the quark part is written explicitly as it will serve as an example. In this form, soft-collinear interactions are present at LP since

$$in_- D = in_- \partial + g_s\, n_- A_c(z) + g_s\, n_- A_s(z_-). \tag{2.3}$$

The n_- component of the soft gluon field is unsuppressed with respect to the corresponding component of the collinear field, resulting in the well-known eikonal form of the soft-collinear interaction. This means diagrams of type shown in figure 2 exist.

The external soft line provides a scale to the collinear loop, and indeed, individually, such diagrams are non-vanishing. Following the labeling in figure 2, k, p, and l are soft, collinear, and anticollinear momenta, respectively. One can then form the collinear invariant $(n_- k)(n_+ p) \sim \lambda^2$, resulting in dimensionally regulated results proportional to $[\mu^2/((n_- k)(n_+ p))]^\epsilon$. It therefore appears that there should be collinear functions already at LP.

However, at LP, the decoupling transformation [31] $\xi_c(z) \to Y_+(z_-)\, \xi_c^{(0)}(z)$, $A_c^\mu(z) \to Y_+(z_-) A_c^{(0)\mu}(z) Y_+^\dagger(z_-)$ can be applied, where the soft Wilson line is defined as

$$Y_\pm\,(x) \,=\, \mathbf{P} \exp\left[i g_s \int_{-\infty}^0 ds\, n_\mp A_s\,(x + s n_\mp) \right]. \tag{2.4}$$

Since

$$\bar{\xi}_c\, in_- D\, \frac{\not{n}_+}{2}\, \xi_c = \bar{\xi}_c^{(0)}\, in_- D_c^{(0)}\, \frac{\not{n}_+}{2}\, \xi_c^{(0)}\,, \tag{2.5}$$

this removes all soft-collinear interactions from the LP Lagrangian (2.2). It is often convenient to define the collinear gauge-invariant field $\chi_c = W_c^\dagger \xi_c$ involving the collinear Wilson line[2]

$$W_c\,(x) \,=\, \mathbf{P} \exp\left[i g_s \int_{-\infty}^0 ds\, n_+ A_c\,(x + s n_+) \right], \tag{2.6}$$

[2]Similar definitions apply to the collinear gluon field, and to anticollinear fields with $n_+ \leftrightarrow n_-$.

JHEP07(2020)078

in which case

$$\bar{\xi}_c\, in_- D\, \frac{\not{n}_+}{2}\, \xi_c = \bar{\chi}_c^{(0)} \left(in_- \partial + n_- \mathcal{A}_c^{(0)} \right) \frac{\not{n}_+}{2}\, \chi_c^{(0)} \tag{2.7}$$

with $\mathcal{A}_c^\mu = W_c^\dagger\, [iD_c^\mu\, W_c]$, and the same conclusion applies. It is customary to drop the superscript (0) on the fields after the decoupling transformation and we follow this convention below.

Returning to the example diagram above, the decoupling transformation implies that after summing together all collinear loop diagrams, they must cancel exactly. This is the reason why there are no collinear functions at LP. The fact that the collinear scale shows up in intermediate steps of the calculation is a consequence of using Feynman rules derived from the SCET Lagrangian before the decoupling transformation. Indeed, if one employed the decoupled Lagrangian, diagrams like the one in figure 2 would not be present from the beginning.

It follows from the absence of soft-collinear interactions at LP after the decoupling transformation that the matrix element relevant to DY production factorizes at LP into a product of (anti)collinear fields and the soft Wilson lines such that it can be written as

$$\begin{aligned}\langle X|\bar{\psi}\,\gamma^\rho \psi(0)|A(p_A)B(p_B)\rangle = \int dt\, d\bar{t}\, \widetilde{C}^{A0,A0}(t,\bar{t}\,)\, \langle X_{\bar{c}}^{\rm PDF}|\bar{\chi}_{\bar{c}}\,(\bar{t}n_-)|B(p_B)\rangle\, \gamma_\perp^\rho \\ \times \langle X_c^{\rm PDF}|\chi_c\,(tn_+)\,|A(p_A)\rangle\, \langle X_s|\mathbf{T}\left(\left[Y_-^\dagger(0)Y_+(0)\right]\right)|0\rangle\,. \end{aligned} \tag{2.8}$$

Here $\widetilde{C}^{A0,A0}(t,\bar{t}\,)$ is the short-distance matching coefficient of the electromagnetic current to its leading-power SCET representation $J_\rho^{A0,A0}(t,\bar{t}\,) = \bar{\chi}_{\bar{c}}(\bar{t}n_-)\gamma_{\perp\rho}\chi_c(tn_+)$. Due to threshold kinematics the final state can only be composed of soft and $(\bar{c})c$-PDF collinear modes, which are decoupled. Hence, in the above equation the final state is factorized, $\langle X| = \langle X_s|\langle X_c^{\rm PDF}|\langle X_{\bar{c}}^{\rm PDF}|$.

Since soft-collinear interactions are absent and purely threshold-collinear loops are scaleless, the matching between the collinear field χ_c and the corresponding c-PDF field $\chi_c^{\rm PDF}$ is trivial: the threshold-collinear fields are simply identified with the c-PDF fields. Technically, the matching coefficient (collinear function) is a delta function to all orders in perturbation theory converting threshold-collinear fields to c-PDF fields, that is,

$$\chi_c(tn_+) = \int du\, \tilde{J}(t,u)\, \chi_c^{\rm PDF}(un_+) \tag{2.9}$$

with $\tilde{J}(t,u) = \delta(t-u)$. Because of this trivial relation, LP collinear functions are not discussed in the context of LP factorization.

After this step, the computation proceeds in the usual manner. Squaring the amplitude and summing over the final state gives the usual PDFs $f_{a/A}(x_a)$ and $f_{b/B}(x_b)$ from the (anti)collinear matrix elements, and one arrives at

$$\frac{d\sigma_{\rm DY}}{dQ^2} = \frac{4\pi\alpha_{\rm em}^2}{3N_c Q^4} \sum_{a,b} \int_0^1 dx_a dx_b\, f_{a/A}(x_a) f_{b/B}(x_b)\, \hat{\sigma}_{ab}(z)\,. \tag{2.10}$$

JHEP07(2020)078

The partonic cross section $\hat{\sigma}_{ab}(z)$ factorizes into a hard function, originating from squaring the hard matching coefficient $\widetilde{C}^{A0,A0}(t,\bar{t}\,)$ in (2.8), and a soft function:

$$\hat{\sigma}(z) = H(Q^2)\, Q S_{\rm DY}(Q(1-z))\,. \tag{2.11}$$

The leading power DY soft function is given by [32]

$$S_{\rm DY}(\Omega) = \int \frac{dx^0}{4\pi}\, e^{i\Omega\, x^0/2}\, \frac{1}{N_c}\, {\rm Tr}\, \langle 0|\bar{\mathbf{T}}(Y_+^\dagger(x^0)Y_-(x^0))\, \mathbf{T}(Y_-^\dagger(0)Y_+(0))|0\rangle\,. \tag{2.12}$$

2.2 Emergence of collinear functions

The analysis becomes more involved when subleading-power effects are studied. The framework employed here for the power-suppressed corrections in SCET was developed in [33–36]. It makes use of collinear gauge-invariant building blocks, which consist of collinear quark and gluon fields in a particular collinear direction, and non-local operators with insertions of terms from the power-suppressed SCET Lagrangian to systematically include subleading-power contributions in perturbative calculations. In what follows, we use this general framework to derive power corrections to the LP factorization formula for DY production at threshold. We find that the new physical ingredients, the collinear functions, arise from soft-collinear interactions present in the power-suppressed Lagrangian. These technically appear as a consequence of Lagrangian insertions in time-ordered product operators.

As an illustrative example, we consider the insertion of the NLP soft-collinear interaction Lagrangian

$$\mathcal{L}^{(2)}_{2\xi}(z) = \frac{1}{2}\, \bar{\chi}_c(z)\, z_\perp^\mu\, z_\perp^\nu \left[i\partial_\nu\, in_-\partial\, \mathcal{B}^+_\mu(z_-)\right] \frac{\not{n}_+}{2}\, \chi_c(z) \tag{2.13}$$

from (A.1). The decoupling transformation has already been performed (and the superscript (0) on the collinear gauge-invariant quark field χ_c dropped), and the $\mathcal{B}_\pm$ field is a soft building block formed by a soft covariant derivative and soft Wilson lines (we also define the soft quark building block for completeness)

$$\mathcal{B}^\mu_\pm = Y_\pm^\dagger\, [i\, D_s^\mu\, Y_\pm]\,, \tag{2.14}$$

$$q^\pm = Y_\pm^\dagger\, q_s\,. \tag{2.15}$$

In contrast to LP, the decoupling transformation does *not* remove completely the soft-collinear interactions. In fact, the insertions of Lagrangian terms appear in non-local operators with an integral over the position of the insertion,

$$J_c^{T2}(t) = i \int d^4z\, \mathbf{T}\left[\chi_c(tn_+)\, \mathcal{L}^{(2)}_{2\xi}(z)\right], \tag{2.16}$$

where the field $\chi_c(tn_+)$ arises from the LP $J^{A0,A0}$ current. See figure 3 for illustration. The collinear fields in (2.13) depend on all components of the z coordinate. The soft $\mathcal{B}_\pm(z_-)$ field on the other hand has dependence only on $z_-^\mu = (n_+z)\frac{n_-^\mu}{2}$ due to multipole expansion, but this dependence links the collinear and soft fields and leads to a collinear invariant for

JHEP07(2020)078

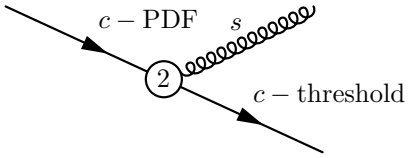

Figure 3. Insertion of the power-suppressed Lagrangian $\mathcal{L}^{(2)}_{2\xi}$ into a collinear quark line.

collinear loop integrals. Concretely, consider the DY matrix element with an insertion of the above Lagrangian,

$$\begin{aligned}\langle X|\bar{\psi}\gamma^\rho\psi(0)|A(p_A)B(p_B)\rangle &= \int dt\, d\bar{t}\, \widetilde{C}^{A0,A0}(t,\bar{t}\,)\, \langle X^{\rm PDF}_{\bar{c}}|\bar{\chi}_{\bar{c},\alpha a}(\bar{t}n_-)|B(p_B)\rangle\gamma^\rho_{\perp,\alpha\gamma} \\ &\times i\int d^4z\, \langle X^{\rm PDF}_c|\frac{1}{2}z^\nu_\perp z^\mu_\perp(in_-\partial_z)^2\, \mathbf{T}\left[\chi_{c,\gamma f}\,(tn_+)\,\bar{\chi}_c\,(z)\,\mathbf{T}^A\frac{\not{n}_+}{2}\chi_c\,(z)\right]|A(p_A)\rangle \\ &\times \langle X_s|\mathbf{T}\left(\left[Y^\dagger_-(0)Y_+(0)\right]_{af}\frac{i\partial^\mu_\perp}{in_-\partial}\mathcal{B}^{+A}_{\perp\nu}\,(z_-)\right)|0\rangle\,. \end{aligned} \tag{2.17}$$

Compared to the LP expression (2.8), there are extra collinear fields in the c-PDF matrix element and there is a convolution in z_- between the soft and collinear matrix elements. It is precisely the presence of this extra convolution, injecting momentum with a soft scaling into the collinear matrix element, which induces a scale and leads to the emergence of collinear functions. The soft matrix element in the last line now contains an explicit gauge field insertion in addition to the Wilson lines, and will form a part of the *generalized* soft function. The anticollinear matrix element is the same as before, and will form part of a parton distribution function (PDF) upon squaring.

We now focus on the collinear matrix element, which appears in the second line. Due to threshold kinematics the threshold-collinear modes are forbidden from entering the final state. At leading power in the Λ/Q expansion, the threshold-collinear fields in the collinear matrix element must be integrated out and matched to c-PDF mode operators consisting of a single quark (or gluon) field, which after squaring the amplitude will lead to the standard PDFs. A prototype for this matching step is the equation (refined later)

$$i\int d^4z\; \mathbf{T}\left[\,\{\psi_c(tn_+)\}\,\mathcal{L}^{(2)}_c(z)\right] = 2\pi\int du\int dz_-\,\tilde{J}(t,u;z_-)\,\chi^{\rm PDF}_c(un_+)\,, \tag{2.18}$$

where $\mathcal{L}^{(2)}_c$ refers to only the collinear pieces of the Lagrangian insertion. The perturbative matching coefficient $\tilde{J}(t,u;z_-)$ is the *collinear function*. It contains the collinear physics at the *amplitude* level. We stress once more that it appears first in power-suppressed corrections to the DY process. The above equation provides an operator definition of the concept of the "radiative jet amplitude" [12, 13, 26]. The matching should be performed in the presence of soft structures which, acting as projectors, define independent collinear functions. We give formal definitions in section 2.3 below.

For the above example, we calculate the tree-level contribution to the collinear terms in the second line of (2.17). To this purpose it is convenient to introduce the momentum-space

JHEP07(2020)078

operator

$$\mathcal{J}^{\mu\nu,\,A}_{\gamma,f}\left(n_+p,\omega\right) \equiv \int dt\, e^{i\,(n_+p)\,t}\, i \int d^4z\, e^{i\omega(n_+z)/2} \times \frac{1}{2} z_\perp^\nu z_\perp^\mu (in_-\partial_z)^2\, \mathbf{T}\left[\chi_{c,\gamma f}\left(tn_+\right)\bar{\chi}_c\left(z\right)\mathbf{T}^A \frac{\not{n}_+}{2}\chi_c\left(z\right)\right], \tag{2.19}$$

which contains only collinear fields. To calculate the perturbative threshold-collinear matching coefficient, we consider the partonic analogue of the matrix element in (2.17), which amounts to replacing the incoming hadron by an incoming quark and the PDF-collinear final state by the vacuum. Hence, we calculate

$$\begin{aligned}\langle 0|\mathcal{J}^{\mu\nu,\,A}_{\gamma,f}\left(n_+q_a,\omega\right)|q(q)_e\rangle &= \int dt e^{i(n_+q_a)\,t}\, i \int d^4z \left[(in_-\partial_z)^2 e^{i\omega\,(n_+z)/2}\right] \\ &\quad \times \frac{1}{2} z_\perp^\nu z_\perp^\mu \langle 0|\mathbf{T}\left[\chi_{c,\gamma f}\left(tn_+\right)\bar{\chi}_c\left(z\right)\mathbf{T}^A \frac{\not{n}_+}{2}\chi_c\left(z\right)\right]|q(q)_e\rangle \\ &= -\frac{1}{2} i\omega^2\,(2\pi)\int \frac{d^4k}{(2\pi)^4}\,\delta\left(n_+q_a - n_+k\right)\int d^4z \left[\frac{\partial}{\partial k_{\perp\nu}}\frac{\partial}{\partial k_{\perp\mu}}\frac{i(n_+k)}{k^2}\right] \\ &\quad \times e^{i\omega\,(n_+z)/2} e^{ik\cdot z}\,\mathbf{T}^A_{fe}\, u_{c,\gamma}(q)\, e^{-iz\cdot q}\,,\end{aligned} \tag{2.20}$$

where we have contracted two of the collinear fields to form the collinear quark propagator, performed the z-derivatives and the integral over t, and used

$$\chi_{c,\gamma d}(z)|q(q)_e\rangle = \delta_{de}\, u_{c,\gamma}(q) e^{-iz\cdot q}\,|0\rangle \tag{2.21}$$

for the incoming quark with fundamental colour index e. The z-integral can next be performed, yielding delta functions which remove the remaining integral over the momentum k. Then we find

$$\langle 0|\mathcal{J}^{\mu\nu,\,A}_{\gamma,f}\left(n_+q_a,\omega\right)|q(q)_e\rangle = (2\pi)\underbrace{\delta\left(n_+q_a - n_+q\right)\frac{-g_\perp^{\nu\mu}}{(n_+q)}\,\mathbf{T}^A_{fe}\,\delta_{\gamma\beta}}_{\equiv J^{\mu\nu,\,A}_{2\xi,\gamma\beta,fe}(n_+q_a,n_+q;\omega)}\, u_{c,\beta}(q)\,. \tag{2.22}$$

We have underbraced the matching coefficient which defines the tree-level collinear function. The appearance of collinear functions beyond LP is generic and constitutes a key concept in NLP investigations. In section 4 we will calculate the one-loop corrections to these functions.

2.3 Collinear matching: formal definitions

The general collinear matching equation, suppressing indices, is given by

$$\begin{aligned} & i^{\,m}\int\{d^dz_j\}\,\mathbf{T}\left[\{\psi_c(t_kn_+)\}\times\left\{\mathcal{L}^{(l)}(z_j)\right\}\right] \\ &\quad = 2\pi\sum_i\int du\int\{dz_{j-}\}\,\tilde{J}_i\left(\{t_k\},u;\{z_{j-}\}\right)\,\chi_c^{\rm PDF}(un_+)\,\mathfrak{s}_i(\{z_{j-}\})\,,\end{aligned} \tag{2.23}$$

where $\{d^dz_j\} = \prod_{j=0}^m d^dz_j$ and $\{dz_{j-}\} = \prod_{j=0}^m \frac{dn_+z_j}{2}$. $\{z_{j-}\}$ denotes the set of m positions at which the soft building block insertions are located. $\left\{\mathcal{L}^{(l)}(z_j)\right\}$ is a set of m

JHEP07(2020)078

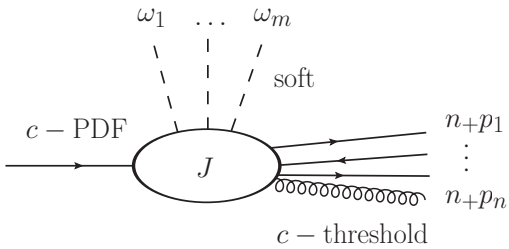

Figure 4. A momentum-space pictorial representation of the matching equation (2.23). The oval labelled J is a collinear function. The ω_i variables are conjugate to the respective positions of the insertions of subleading-power Lagrangians. Many threshold-collinear fields may join to the (possibly power-suppressed) SCET currents of the $A, B, C\ldots$ type [34], but there is only a single c-PDF field at leading twist in the Λ/Q expansion.

$\mathcal{O}(\lambda^l)$-suppressed Lagrangian insertions. $\{\psi_c(t_k n_+)\}$ denotes a set of n fields chosen from the elementary collinear-gauge-invariant collinear building blocks each dependent on one variable from the n-sized set $\{t_k\}$. Here

$$\psi_i(t_i n_{i+}) \in \begin{cases} \chi_i(t_i n_{i+}) \equiv W_i^\dagger\, \xi_i & \text{collinear quark} \\ \mathcal{A}^\mu_{i\perp}(t_i n_{i+}) \equiv W_i^\dagger \left[i\, D^\mu_{i\perp}\, W_i\right] & \text{collinear gluon} \end{cases} \tag{2.24}$$

for the collinear quark and gluon field in i-th direction, respectively. Furthermore, $\mathfrak{s}_i(\{z_{j-}\})$ is a soft operator and the sum over i runs over a basis of soft structures,

$$\begin{aligned} \mathfrak{s}_i(\{z_{j-}\}) \;\in\; \Bigg\{ & \frac{i\partial^\mu_\perp}{in_-\partial}\mathcal{B}^+_{\mu_\perp}(z_{1-}), \frac{i\partial_{[\mu_\perp}}{in_-\partial}\mathcal{B}^+_{\nu_\perp]}(z_{1-}), \\ & \frac{1}{(in_-\partial)^2}\left[\mathcal{B}^{+\,\mu_\perp}(z_{1-}), \left[in_-\partial\mathcal{B}^+_{\mu_\perp}(z_{1-})\right]\right] \;, \frac{1}{(in_-\partial)}\left[\mathcal{B}^+_{\mu_\perp}(z_{1-}), \mathcal{B}^+_{\nu_\perp}(z_{1-})\right], \\ & \mathcal{B}^+_{\mu_\perp}(z_{1-})\mathcal{B}^+_{\nu_\perp}(z_{2-}), \frac{1}{(in_-\partial_{z_1})(in_-\partial_{z_2})} q_{+\sigma}(z_{1-})\bar{q}_{+\lambda}(z_{2-}), \ldots \Bigg\}. \end{aligned} \tag{2.25}$$

Here $[\mu,\nu]$ denotes antisymmetrization $\mu\nu - \nu\mu$, and the ellipses indicate all possible *independent* soft structures[3] after utilizing the equation of motion

$$\begin{aligned} n_+\mathcal{B}^+(z_-) = & -2\frac{i\partial^\mu_\perp}{in_-\partial}\mathcal{B}^+_{\mu_\perp}(z_-) - 2\frac{1}{(in_-\partial)^2}\left[\mathcal{B}^{+\,\mu_\perp}(z_-), \left[in_-\partial\mathcal{B}^+_{\mu_\perp}(z_-)\right]\right] \\ & -2\frac{g_s^2}{(in_-\partial)^2}\mathbf{T}^A\,\bar{q}_+(z_-)\mathbf{T}^A\not{n}_- q_+(z_-). \end{aligned} \tag{2.26}$$

Eq. (2.23) is a formal all-order and all-power matching equation, and it will be used extensively in the following sections. A graphical illustration is given in figure 4.

[3]The list (2.25) is still partially redundant. For later convenience, we have kept the two-gluon soft structures in the second line, although they can be considered as special cases of the bi-local structure $\mathcal{B}^+_{\mu_\perp}(z_{1-})\mathcal{B}^+_{\nu_\perp}(z_{2-})$.

JHEP07(2020)078

3 Factorization near threshold

We now turn to the formal derivation of the factorization formula beyond leading power. We recall that the SCET derivation of factorization at LP [5] involves matching the coupling to the virtual photon to the LP SCET current,

$$\bar{\psi}\gamma_\rho\psi(0) = \int dt\, d\bar{t}\, \widetilde{C}^{A0,A0}(t,\bar{t}\,)\, J_\rho^{A0,A0}(t,\bar{t}\,) \tag{3.1}$$

where (prior to use of decoupling transformation [31])

$$J_\rho^{A0,A0}(t,\bar{t}\,) = \bar{\chi}_{\bar{c}}(\bar{t}n_-)\gamma_{\perp\rho}\chi_c(tn_+)\,. \tag{3.2}$$

The matching coefficient is related to the corresponding momentum-space coefficient by

$$C^{A0,A0}(n_+p, n_-\bar{p}\,) = \int dt\, d\bar{t}\, e^{-i\,(n_+p)\,t - i\,(n_-\bar{p})\,\bar{t}}\;\widetilde{C}^{A0,A0}(t,\bar{t}\,)\,. \tag{3.3}$$

The fields, denoted by χ_c (and $\mathcal{A}^\mu_{c\perp}$ further on), are the collinear-gauge-invariant collinear quark (and gluon) fields out of which building blocks of general N-jet operators are formed [34]. To derive the factorization formula valid at subleading powers, the matching equation (3.1) must be modified to include higher orders in the $(1-z)$ expansion. In general, this is accomplished through inclusion of all possible combinations of power-suppressed currents and subleading Lagrangian insertions. We obtain such general factorization formula in the following, before specializing to the case of NLP in later sections where we provide explicit results for the objects appearing in the factorization formula.

3.1 Factorization at general subleading powers

Omitting the index structure for clarity, the general, all power, hard matching of the vector current is given by

$$\bar{\psi}\gamma_\rho\psi(0) = \sum_{m_1,m_2} \int \{dt_k\}\,\{d\bar{t}_{\bar{k}}\}\,\widetilde{C}^{\,m_1,m_2}\left(\{t_k\},\,\{\bar{t}_{\bar{k}}\}\right)\,J_s(0)\,J_\rho^{m_1,m_2}\left(\{t_k\},\,\{\bar{t}_{\bar{k}}\}\right)\,. \tag{3.4}$$

The sizes of the sets $\{dt_k\}$, $\{t_k\}$ (and the barred sets for the anticollinear direction) for each term on the right-hand side of the matching equation depend on the type of current present in that term. Inclusion of all contributions is accounted for by the sum over indices m_1 and m_2, which label the basis of SCET operators (and their corresponding short-distance matching coefficients $\widetilde{C}^{\,m_1m_2}$) depending on the content of its building blocks using the formalism and notation developed in [34, 35], for example $m_{1,2} = A0$ in the LP case (3.1). Explicitly, the DY process consists of a collinear and an anticollinear direction both of which can contain sources of power suppression, hence the SCET currents are built as follows

$$J_\rho^{m_1,m_2}\left(\{t_k\},\,\{\bar{t}_{\bar{k}}\}\right) = J_{\bar{c}}^{m_1}\left(\{\bar{t}_{\bar{k}}\}\right)\,\Gamma_\rho^{m_1,m_2}\,J_c^{m_2}\left(\{t_k\}\right)\,. \tag{3.5}$$

As mentioned above, $J_c^{m_2}\left(\{t_k\}\right)$ is constructed using collinear-gauge-invariant collinear building blocks given in (2.24). In this general construction, the letter A, B, C etc. used

JHEP07(2020)078

to label the operator denotes the number of fields in a particular collinear direction, and the number 0, 1, 2 etc. denotes the overall power of λ of the current with respect to the LP, which is labelled 0. Hence, the A-type current consists of one field in one direction and derivatives of that field, the B-type current contains two fields and their derivatives, and so on. $\Gamma_\rho^{m_1,m_2}$ in (3.5) stands for the appropriate spinor and Lorentz structure of the operator. For instance, in (3.2) $\Gamma_\rho^{A0,A0} = \gamma_{\perp\rho}$. At $\mathcal{O}(\lambda)$, $\Gamma_\rho^{A0,A1} = n_{+\rho}$ etc.

In addition, there exist time-ordered products of currents with subleading terms in the SCET Lagrangian. These are denoted by Tn, for example

$$J_c^{T2}(t) = i \int d^d z \, \mathbf{T} \left[J_c^{A0}(t) \, \mathcal{L}^{(2)}(z) \right] \tag{3.6}$$

at $\mathcal{O}(\lambda^2)$, where $\mathcal{L}^{(2)} = \mathcal{L}_\xi^{(2)} + \mathcal{L}_{\xi q}^{(2)} + \mathcal{L}_{\rm YM}^{(2)}$ are the power-suppressed terms in the SCET Lagrangian [29]. As discussed in section 2, the decoupling transformation does not remove the soft-collinear interactions in the subleading SCET Lagrangian and the injection of soft momentum into collinear loops is necessary to form non-vanishing collinear functions. For this reason the time-ordered product terms are crucial ingredients of the factorization of the DY process at NLP. To yield a non-zero subleading power amplitude at least one leg must have such time-ordered product. The other leg can then contribute to power suppression through power-suppressed currents of A, B, C etc. type or another operator containing a time-ordered product. Starting from $\mathcal{O}\left(\lambda^3\right)$, in addition to collinear fields, the current operator can contain purely soft building blocks [34], denoted by $J_s(0)$ here.

As discussed above, only the ($\bar{c}$)c-PDF modes can be radiated into the final state. Eq. (3.5), however, contains threshold (anti)collinear modes, hence a second collinear matching onto a ($\bar{c}$)c-PDF field must be performed using (2.23). The first line of (2.23) corresponds to the time-ordered product of the collinear part $J_c^{m_2}(\{t_k\})$ of a general SCET operator (3.5) with a subleading-power Lagrangian, hence applying (2.23) to the collinear and anticollinear sectors, we obtain the DY matrix element of (3.4) in the form

$$\begin{aligned}
\langle X|\bar{\psi}\gamma_\rho\psi(0)|A(p_A)B(p_B)\rangle = & \sum_{m_1,m_2} \sum_{i,\bar{i}} \int \{dt_k\}\,\{d\bar{t}_{\bar{k}}\}\, \widetilde{C}^{\,m_1,m_2}\left(\{t_k\},\,\{\bar{t}_{\bar{k}}\}\right) \\
& \times 2\pi \int d\bar{u} \int \{d\bar{z}_{\bar{j}+}\}\, \bar{\tilde{J}}_{\bar{i}}^{m_1}\left(\{\bar{t}_{\bar{k}}\}, \bar{u}; \{\bar{z}_{\bar{j}+}\}\right) \langle X_{\bar{c}}^{\rm PDF}|\bar{\chi}_{\bar{c}}^{\rm PDF}(\bar{u}n_-)|B(p_B)\rangle \\
& \times 2\pi \int du \int \{dz_{j-}\}\, \tilde{J}_i^{m_2}\left(\{t_k\}, u; \{z_{j-}\}\right) \langle X_c^{\rm PDF}|\chi_c^{\rm PDF}(un_+)|A(p_A)\rangle \\
& \times \Gamma_\rho^{m_1,m_2} \langle X_s|\, \mathbf{T}\left(\bar{\mathfrak{s}}_{\bar{i}}\left(\{\bar{z}_{\bar{j}+}\}\right)\left[Y_-^\dagger\, J_s\, Y_+\right](0)\, \mathfrak{s}_i\left(\{z_{j-}\}\right)\right)|0\rangle\,.
\end{aligned} \tag{3.7}$$

In this equation, the index k ($\bar{k}$) counts the number of building block fields in the collinear (anticollinear) direction within each current, and we sum over all currents. The index j ($\bar{j}$) refers to the number of Lagrangian insertions in the collinear (anticollinear) sector, where we also sum over all possibilities. Note that here, and throughout the text, the barred notation ($^-$) refers to the anticollinear direction, and the tilde ($\tilde{}$) is used to denote the quantities with dependence on the position arguments such as $t, \bar{t}$ and so on. This notation, also used for indices, is meant to facilitate keeping track of the origin of the various contributions to the factorization theorem. As discussed in section 2 at least one

JHEP07(2020)078

Lagrangian insertion is necessary to yield a non-vanishing subleading-power amplitude. Finally, the $\tilde{J}_i$ ($\bar{\tilde{J}}_{\bar{i}}$) are the (anti)collinear functions and $\mathfrak{s}_i(\{z_{j-}\})$ ($\bar{\mathfrak{s}}_{\bar{i}}(\{\bar{z}_{\bar{j}+}\})$) are made up of explicit $\mathcal{B}^+$, q_+ ($\mathcal{B}^-$, q_-) field products and their derivatives, as indicated in (2.25).[4] The further derivation of the general factorization formula follows closely the steps presented in [14] for the derivation of the NLP leading logarithmic resummation. Suppressing the $m_{1,2}$ labels, the hard matching coefficients and c-PDF fields are Fourier-transformed using

$$\widetilde{C}\left(\{t_k\},\{\bar{t}_{\bar{k}}\}\right) = \int \left\{\frac{dn_+p_k}{2\pi}\right\}\left\{\frac{dn_-\bar{p}_{\bar{k}}}{2\pi}\right\} e^{i\,(n_+p_k)\,t_k} e^{i\,(n_-\bar{p}_{\bar{k}})\,\bar{t}_{\bar{k}}}\, C(\{n_+p_k\},\{n_-\bar{p}_{\bar{k}}\}) \tag{3.8}$$

and

$$\chi_c^{\rm PDF}(un_+) = \int \frac{d(n_+p_a)}{2\pi} e^{-i(n_+p_a)\,u}\,\hat{\chi}_c^{\rm PDF}(n_+p_a)\,, \tag{3.9}$$

respectively. For the collinear functions we define ($z_{j-} = n_+z_j/2$)

$$\begin{aligned}&\int\{dt_k\}\int du\,\tilde{J}_i^{m_2}\left(\{t_k\},u;\{z_{j-}\}\right)\,e^{i\,(n_+p_k)\,t_k}\,e^{-i(n_+p_a)\,u}\\ &\quad= \int\left\{\frac{d\omega_j}{2\pi}\right\}\,e^{-i\omega_j\,z_{j-}}\,J_i^{m_2}\left(\{n_+p_k\},n_+p_a;\{\omega_j\}\right)\,.\end{aligned} \tag{3.10}$$

The set $\{\omega_j\}$ is a set of variables with soft scaling conjugate to $\{z_{j-}\}$, and $\left\{\frac{d\omega_j}{2\pi}\right\} = \frac{d\omega_1}{2\pi}\times\ldots\times\frac{d\omega_m}{2\pi}$. Einstein's summation convention is implied in the exponents. Equations analogous to (3.9) and (3.10) are used for the anticollinear direction. Implementing these in (3.7) we arrive at generalized version of eq. (3.16) of [14]:

$$\begin{aligned}\langle X|\bar{\psi}\gamma_\rho\psi(0)|A(p_A)B(p_B)\rangle &= \sum_{m_1,m_2}\sum_{i,\bar{i}}\int\left\{\frac{dn_+p_k}{2\pi}\right\}\left\{\frac{dn_-\bar{p}_{\bar{k}}}{2\pi}\right\}\\ &\times\int d(n_+p_a)\;d(n_-p_b)\,C^{\,m_1,m_2}(\{n_+p_k\},\,\{n_-\bar{p}_{\bar{k}}\})\\ &\times\int\left\{\frac{d\bar{\omega}_{\bar{j}}}{2\pi}\right\}\,\bar{J}_{\bar{i}}^{m_1}\left(\{n_-\bar{p}_{\bar{k}}\},-n_-p_b;\,\{\bar{\omega}_{\bar{j}}\}\right)\;\langle X_{\bar{c}}^{\rm PDF}|\hat{\bar{\chi}}_{\bar{c}}^{\rm PDF}(n_-p_b)|B(p_B)\rangle\\ &\times\int\left\{\frac{d\omega_j}{2\pi}\right\}\,J_i^{m_2}\left(\{n_+p_k\},n_+p_a;\,\{\omega_j\}\right)\,\langle X_c^{\rm PDF}|\hat{\chi}_c^{\rm PDF}(n_+p_a)|A(p_A)\rangle\\ &\times\Gamma_\rho^{m_1,m_2}\int\{d\bar{z}_{\bar{j}+}\}\int\{dz_{j-}\}\,e^{-i\bar{\omega}_{\bar{j}}\,\bar{z}_{\bar{j}+}}\;e^{-i\omega_j\,z_{j-}}\\ &\times\langle X_s|\,\mathbf{T}\left(\bar{\mathfrak{s}}_{\bar{i}}\left(\{\bar{z}_{\bar{j}+}\}\right)\left[Y_-^\dagger\,J_s\,Y_+\right](0)\,\mathfrak{s}_i(\{z_{j-}\})\right)|0\rangle\,.\end{aligned} \tag{3.11}$$

For brevity, we define the coefficient function

$$\begin{aligned}D_{i\bar{i}\,\rho}^{\,m_1,m_2}\left(n_+p_a,-n_-p_b;\{\omega_j\},\{\bar{\omega}_{\bar{j}}\}\right) &= (2\pi)^2\int\left\{\frac{dn_+p_k}{2\pi}\right\}\left\{\frac{dn_-\bar{p}_{\bar{k}}}{2\pi}\right\}\\ &\times C^{\,m_1,m_2}(\{n_+p_k\},\{n_-\bar{p}_{\bar{k}}\})\,\bar{J}_{\bar{i}}^{m_1}(\{n_-\bar{p}_{\bar{k}}\},-n_-p_b;\{\bar{\omega}_{\bar{j}}\})\\ &\times\Gamma_\rho^{m_1,m_2}\;J_i^{m_2}(\{n_+p_k\},n_+p_a;\{\omega_j\})\end{aligned} \tag{3.12}$$

that contains both, the hard and collinear matching functions at the amplitude level.

[4] To be precise, at leading power and when only one time-ordered product is present, both or one of the collinear functions are trivial and the corresponding soft structure is unity.

JHEP07(2020)078

The next step in the derivation of the factorization formula is to square the amplitude, which gives the hadronic tensor $W_{\mu\rho}$ defined below. Combined with the transverse lepton tensor belonging to the final-state lepton pair, for which the phase-space integrals are computed in d dimensions, we obtain an expression for the cross section

$$d\sigma = \frac{4\pi\alpha_{\rm em}^2}{3s\,q^2}\frac{d^dq}{(2\pi)^d}\left(-g^{\mu\rho}W_{\mu\rho}\right), \tag{3.13}$$

where

$$\begin{aligned} g^{\mu\rho}W_{\mu\rho} &= \int d^dx\, e^{-iq\cdot x}\,\langle A(p_A)B(p_B)|J^{\dagger\,\rho}(x)J_\rho(0)|A(p_A)B(p_B)\rangle \\ &= \sum_X (2\pi)^d\delta^{(d)}\left(p_A+p_B-q-p_{X_s}-p_{X_c^{\rm PDF}}-p_{X_{\bar c}^{\rm PDF}}\right) \\ &\quad\times\langle A(p_A)B(p_B)|J_\rho^\dagger(0)|X\rangle\langle X|J^\rho(0)|A(p_A)B(p_B)\rangle\,. \end{aligned} \tag{3.14}$$

At this point we transform the c-PDF fields back to coordinate space and use the standard definition

$$\begin{aligned} &\langle A(p_A)|\bar\chi_{c,\eta i}^{\rm PDF}(x+g'n_+)\chi_{c,\beta b}^{\rm PDF}(gn_+)|A(p_A)\rangle \\ &\quad= \frac{\delta_{bi}}{N_c}\left(\frac{\not n_-}{4}\right)_{\beta\eta}(n_+p_A)\int_0^1 dx_a\, e^{i(x+g'n_+-gn_+)\cdot p_Ax_a}\, f_{a/A}(x_a) \end{aligned} \tag{3.15}$$

for the PDF. After performing the integrations over n_+p_a, n_-p_b and some further manipulations, we extract the convolution with the PDFs from the hadronic DY spectrum (2.10), and obtain the expression

$$\begin{aligned} \hat\sigma = &\sum_{\substack{m_1',m_2'\\ m_1,m_2}}\sum_{\substack{i',\bar i'\\ i,\bar i}}\int\left\{\frac{d\bar\omega'_{\bar j'}}{2\pi}\right\}\left\{\frac{d\omega'_{j'}}{2\pi}\right\}\left\{\frac{d\bar\omega_{\bar j}}{2\pi}\right\}\left\{\frac{d\omega_j}{2\pi}\right\} \\ &\times(-Q^2)\left[\left(\frac{\not n_-}{4}\right)D^{*\,m_1',m_2'\,\rho}_{i'\,\bar i'}(x_an_+p_A,x_bn_-p_B;\,\{\omega'_{j'}\},\,\{\bar\omega'_{\bar j'}\})\right. \\ &\left.\times\left(\frac{\not n_+}{4}\right)D^{m_1,m_2}_{i\,\bar i\,\rho}(x_an_+p_A,x_bn_-p_B;\{\omega_j\},\,\{\bar\omega_{\bar j}\})\right] \\ &\times\int\frac{d^{d-1}\vec q}{(2\pi)^{d-1}\,2\sqrt{Q^2+\vec q^{\,2}}}\,\frac{1}{2\pi}\int d^dx\, e^{i(x_ap_A+x_b\,p_B-q)\cdot x} \\ &\times\widetilde S_{i\,\bar i\,i'\,\bar i'}(x;\{\omega_j\},\{\bar\omega_{\bar j}\},\{\omega'_{j'}\},\{\bar\omega'_{\bar j'}\}) \end{aligned} \tag{3.16}$$

for the $q\bar q$-induced partonic cross section near threshold including power corrections in $(1-z)$ in the most general form. We recall that barred notation refers to the anticollinear direction, and the tilde denotes objects which depend on position-space arguments. Contributions to the factorization formula from the complex conjugate amplitude are marked here and throughout the text with a prime ($'$) symbol. This notation persists in the indices and is used in combination with each other, such that $\bar i'$ refers to contribution from the anticollinear part of the complex conjugate amplitude. In the last line we introduced the

JHEP07(2020)078

generalized multi-local soft function, $\widetilde{S}_{i\bar{\imath}i'\bar{\imath}'}(x;\{\omega_j\},\{\bar{\omega}_{\bar{\jmath}}\},\{\omega'_{j'}\},\{\bar{\omega}'_{\bar{\jmath}'}\})$, defined as

$$\begin{aligned}
&\widetilde{S}_{i\bar{\imath}i'\bar{\imath}'}(x;\{\omega_j\},\{\bar{\omega}_{\bar{\jmath}}\},\{\omega'_{j'}\},\{\bar{\omega}'_{\bar{\jmath}'}\}) \\
&\quad= \int\{d\bar{z}'_{\bar{\jmath}'+}\}\int\{dz'_{j'-}\}\int\{d\bar{z}_{\bar{\jmath}+}\}\int\{dz_{j-}\}\; e^{+i\bar{\omega}'_{\bar{\jmath}'}\bar{z}'_{\bar{\jmath}'+}}\, e^{+i\omega'_{j'}z'_{j'-}}\; e^{-i\bar{\omega}_{\bar{\jmath}}\bar{z}_{\bar{\jmath}+}}\; e^{-i\omega_j z_{j-}} \\
&\qquad\times\frac{1}{N_c}\,\mathrm{Tr}\,\langle 0|\bar{\mathbf{T}}\left(\bar{\mathfrak{s}}'_{i'}\left(\{x+z'_{j'-}\}\right)\left[Y_+^\dagger\, J_s^\dagger\, Y_-\right](x)\,\mathfrak{s}'_{i'}\left(\{x+\bar{z}'_{\bar{\jmath}'+}\}\right)\right) \\
&\qquad\times\mathbf{T}\left(\bar{\mathfrak{s}}_{\bar{\imath}}\left(\{\bar{z}_{\bar{\jmath}+}\}\right)\left[Y_-^\dagger\, J_s\, Y_+\right](0)\,\mathfrak{s}_i\left(\{z_{j-}\}\right)\right)|0\rangle\,.
\end{aligned} \tag{3.17}$$

This concludes the derivation of the general formula for the DY cross section near threshold including power corrections. Note that these results were stated in eqs. (2.1) and (2.2) of [14] without details, which are given here.

3.2 Factorization at NLP

We next focus on the next-to-leading power effects where certain simplifications in the general formula (3.16) can be made. We first note that since the ω variables are connected to the soft emissions from collinear functions, and therefore come from insertions of subleading-power Lagrangians in a time-ordered product, at NLP their total number is highly constrained. On the one hand, there must be at least one ω present due to the fact that at least one time-ordered product operator must appear in the SCET amplitude in order to provide a threshold-collinear scale and not lead to a trivial null result, as explained earlier in the text. On the other hand, the total power suppression at NLP is $\mathcal{O}(\lambda^2)$, which means that there can be at most two separate ω variables which correspond to two $\mathcal{L}^{(1)}$ insertions, each contributing $\mathcal{O}(\lambda)$ suppression. The constraint on the number of subleading power interactions also limits the number of soft structures $\mathfrak{s}_i$ from the set (2.25), required at NLP.

In the position-space SCET framework, soft fields in the current operators appear only from $\mathcal{O}(\lambda^3)$ [34]. Hence, at NLP, the soft part $J_s(0)$ is not present, and the soft structures come only from single insertions of the $\mathcal{O}(\lambda^2)$ SCET Lagrangian, $\mathcal{L}_\xi^{(2)}$ and $\mathcal{L}_{\mathrm{YM}}^{(2)}$, and double insertions of the single power-suppressed terms, $\mathcal{L}_\xi^{(1)}$, $\mathcal{L}_{\xi q}^{(1)}$, and $\mathcal{L}_{\mathrm{YM}}^{(1)}$.

The next simplification is due to the fact that the kinematics of the process in the centre-of-mass frame does not support power suppression created by a single operator with $\mathcal{O}(\lambda)$ scaling on a given leg. This is because the incoming collinear momentum can be chosen to carry only its large component, $n_+p \sim Q$ ($n_-l \sim Q$ for the anticollinear leg), and all components of soft momentum scale as $\mathcal{O}(\lambda^2)$. For the (anti)collinear direction to carry $\mathcal{O}(\lambda)$ suppression, it would necessarily have to be proportional to the transverse component of the (anti)collinear vector, $p_\perp^\mu(l_\perp^\mu) \sim Q\lambda$, since no other momentum component in the threshold kinematics carries $\mathcal{O}(\lambda)$ scaling, which, however, vanishes. This means that the $\mathcal{O}(\lambda^2)$ power suppression cannot come from two insertions of $\mathcal{L}_\xi^{(1)}$ (or $\mathcal{L}_{\mathrm{YM}}^{(1)}$) on two separate legs of a diagram. Moreover, a non-vanishing $\mathcal{O}(\lambda)$ *amplitude* also cannot exist in the $q\bar{q}$ channel.[5] In consequence, at cross section level at NLP, the $\mathcal{O}(\lambda^2)$ suppression

[5]Soft quark emission does yield a non-vanishing $\mathcal{O}(\lambda)$ amplitude, however this contributes to the (anti)quark-gluon (qg, $\bar{q}g$) channel.

JHEP07(2020)078

must be generated in the amplitude which then interferes with the LP amplitude according to (3.14), yielding the $\mathcal{O}(\lambda^2)$ suppressed cross section. This still leaves the possibility of $\mathcal{O}(\lambda^2)$ suppression to be generated by the $J^{T2}(t)$ operator formed by a $\mathcal{L}^{(1)}$ insertion and a subleading current of $A1$ or $B1$-type. Due to chirality and helicity conservation in QCD, the possible currents are

$$J_\rho^{A0,A1}(t,\bar{t}\,) = \bar{\chi}_{\bar{c}}(\bar{t}n_-)\, n_{+\rho}\, i\partial\!\!\!/_\perp \chi_c(tn_+), \tag{3.18}$$

$$J_\rho^{A0,B1}(t_1,t_2,\bar{t}\,) = \bar{\chi}_{\bar{c}}(\bar{t}n_-)\, n_{\pm\rho}\, A\!\!\!/_{\perp c}(t_2 n_+)\chi_c(t_1 n_+), \tag{3.19}$$

and corresponding ones with power suppression in the anticollinear direction. The important detail to note is that both currents are each proportional to $n_{\pm\rho}$. However, the power-suppressed amplitude in which these currents could appear, is interfered with the LP amplitude, which is proportional to $\gamma_{\perp\rho}$, as can be seen in (3.2). Contraction of these two structures makes such contribution vanish at the cross section level to all orders in perturbation theory. This means that at NLP the sum over indices in $m_{1,2}$ in the formula derived in section 3.1 contains only the $A0$-type current, along with time-ordered products of the LP current with Lagrangian insertions. Hence, only the hard matching coefficient $C^{\,A0,A0}$ of the LP current appears in the NLP factorization formula.

These considerations lead to the conclusion that the soft structures relevant at NLP are in fact the terms already explicitly presented in (2.25) (dropping the ellipsis) after the use of the equation of motion to eliminate the redundant $n_+\mathcal{B}^+$ structure.

The simplifications outlined above make it possible to write down a NLP version of the general subleading-power factorization formula (3.16) in a more compact way. Namely, up to NLP (3.16) simplifies to

$$\begin{aligned}\hat{\sigma}(z) = \sum_{i,i'=0}^{5} \int \left\{\frac{d\omega_j}{2\pi}\right\}\left\{\frac{d\omega'_{j'}}{2\pi}\right\} \mathrm{Tr}\Bigg[\left(\frac{n\!\!\!/_-}{4}\right) D^{*\,\rho}_{i'}(x_a n_+ p_A, x_b n_- p_B; \{\omega'_{j'}\}) \\ \times \left(\frac{n\!\!\!/_+}{4}\right) D_{i\rho}(x_a n_+ p_A, x_b n_- p_B; \{\omega_j\})\Bigg] \\ \times (-Q^2) \int \frac{d^{d-1}\vec{q}}{(2\pi)^{d-1}\, 2\sqrt{Q^2+\vec{q}^{\,2}}}\, \frac{1}{2\pi} \int d^d x\, e^{i(x_a p_A + x_b p_B - q)\cdot x}\, \widetilde{S}_{ii'}\,(x;\{\omega_j\},\{\omega'_{j'}\}) \\ + \bar{c}\text{-terms}\,,\end{aligned} \tag{3.20}$$

The set notation, with $\{\omega_j\} = \{\omega_1, \omega_2\}$, is only required for terms $i = 4, 5$ where the soft structures consist of insertions of fields at different positions, as can be seen in the explicit expressions below. All other terms require only a single ω variable, aside from the LP position-space soft function

$$\widetilde{S}_0(x) = \frac{1}{N_c}\mathrm{Tr}\,\langle 0|\bar{\mathbf{T}}\left[Y_+^\dagger(x)Y_-(x)\right]\mathbf{T}\left[Y_-^\dagger(0)Y_+(0)\right]|0\rangle\,. \tag{3.21}$$

In (3.20) the terms with power suppression placed on the anticollinear leg, both in the amplitude and its conjugate, are indicated by "$\bar{c}$-terms" and not written explicitly, since eventually they contribute a factor of 2 to the power-suppressed terms in the above formula.

JHEP07(2020)078

As explained above, the general structure Γ^ρ defined in (3.5) is simply $\gamma_\perp^\rho$ at NLP, since only the $J^{A0,A0}$ current needs to be used in time-ordered products with Lagrangian insertions in the matching to the DY current. Furthermore, the anticollinear functions $\bar{J}_{\bar{i}}^{m_1}(\{n_-\bar{p}_{\bar{k}}\}, -n_-p_b; \{\bar{\omega}_{\bar{j}}\})$ in the general definition (3.12) are delta functions in $D_{i\rho}(x_a n_+p_A, x_b n_-p_B; \{\omega_j\})$, which therefore simplify to[6]

$$D_{i\rho}(x_a n_+p_A, x_b n_-p_B;\, \{\omega_j\}\,) = \int d(n_+p)\, d(n_-\bar{p})\; C^{A0,A0}(n_+p, n_-\bar{p}) \\ \times \delta(n_-\bar{p} - x_b\, n_-p_B)\, \gamma_{\perp\rho}\, J_i\,(n_+p, x_a\, n_+p_A; \{\omega_j\})\ . \quad (3.22)$$

The index i, which is summed over in (3.20), stands in place of all indices — Dirac, Lorentz, and colour — required by each term depending on the specific soft structure appearing in the collinear matching (2.23). It is understood that one should perform the contraction of these indices prior to the spin trace in (3.20), because some soft functions, for example S_5 below, can have open spin indices which are connected to the collinear function. An expression similar to (3.22) with $\{\omega'_{j'}\}$ variables holds for the conjugate amplitude.

Eq. (3.20) still contains the unexpanded final-state phase-space integral over the lepton-pair momentum $\vec{q}$. This means that in addition to the dynamical power corrections to the amplitude, there is a kinematic power correction from the phase-space integration over the LP amplitude, which will be discussed in more detail below.

Next, we would like to draw attention to the collinear functions themselves. Since, as noted above, at NLP only the LP current $J^{A0,A0}$ is needed in time-ordered products with Lagrangian insertions, the set $\{\psi_c(t_k n_+)\}$ in the general collinear matching equation (2.23) consists of a single quark (or antiquark) collinear field, and the set $\{\mathcal{L}^{(l)}(z_j)\}$ of Lagrangian insertions is either $\{\mathcal{L}^{(2)}(z)\}$ or $\{\mathcal{L}^{(1)}(z_1), \mathcal{L}^{(1)}(z_2)\}$. We also use momentum-space collinear functions as defined in (3.10), hence the collinear matching equation at NLP is either

$$i\int d^4z\, \mathbf{T}\Big[\chi_{c,\gamma f}\,(tn_+)\;\mathcal{L}^{(2)}(z)\Big] = 2\pi\sum_i \int\frac{d\omega}{2\pi}\int\frac{dn_+p}{2\pi}\, e^{-i\,(n_+p)\,t}\int\frac{dn_+p_a}{2\pi} \\ \times J_{i;\gamma\beta,\mu,fbd}\,(n_+p, n_+p_a;\omega)\;\hat{\chi}^{\rm PDF}_{c,\beta b}\,(n_+p_a)\int dz_-\, e^{-i\,\omega\, z_-}\,\mathfrak{s}_{i;\mu,d}(z_-)\,, \quad (3.23)$$

or the one with two $\mathcal{L}^{(1)}$ insertions, in which case the collinear function (soft function) has two arguments $\{\omega_1, \omega_2\}$ ($\{z_{1-}, z_{2-}\}$) and the corresponding integrations must be added. The indices μ and d carried by $\mathfrak{s}$ represent the collective Lorentz and colour indices appropriate for the given soft structure. For each independent soft structure $\mathfrak{s}_i$ there exists a corresponding collinear function J_i as shown on the right-hand side of the above equation.

Thus far we have focused on the derivation of the factorization formula for the bare partonic cross section $\hat{\sigma}$. Indeed, $\hat{\sigma}$ still contains collinear singularities, which are usually subtracted by PDF renormalization. Therefore, care has to be taken when dealing with this d-dimensional quantity. For instance, the spin trace which appears at leading power gives a factor $\mathrm{Tr}\left[\left(\frac{\not{n}_-}{4}\right)\gamma_{\perp\rho}\left(\frac{\not{n}_+}{4}\right)\gamma_\perp^\rho\right] = -(1-\epsilon)$. In order to compare with with literature

[6] At LP, collinear and anticollinear functions are delta functions, and $D_{i\rho}$ reduces to $\gamma_{\perp\rho}\, C^{A0,A0}$.

JHEP07(2020)078

we find it convenient to consider the quantity $\Delta(z)$ defined through

$$\Delta(z) = \frac{1}{(1-\epsilon)} \frac{\hat{\sigma}(z)}{z}\,, \tag{3.24}$$

with the factor $(1-\epsilon)$ divided out compared to [37].

We next simplify the factorization formula in (3.20) further by discussing separately the kinematic and dynamical NLP correction.

3.2.1 NLP kinematic correction $\Delta^{\rm kin}_{\rm NLP}(z)$

In the partonic centre-of-mass frame of the DY process, where $x_a\,\vec{p}_A + x_b\,\vec{p}_B = 0$, the three-momentum of the DY boson has to be balanced by the soft radiation, $\vec{q} = -\vec{p}_{X_s}$. The soft radiation energy is expanded in powers of λ as follows:

$$\big(x_a p_A + x_b p_B - q\big)^0 = p^0_{X_s} = \sqrt{\hat{s}} - \sqrt{Q^2 + \vec{q}^{\,2}} = \frac{\Omega_*}{2} - \frac{\vec{q}^{\,2}}{2Q} + \mathcal{O}(\lambda^6)\,, \tag{3.25}$$

where the first term has a further expansion in $(1-z)$,

$$\Omega_* = \frac{2\,Q(1-\sqrt{z})}{\sqrt{z}} = Q\,(1-z) + \frac{3}{4}\,Q\,(1-z)^2 + \mathcal{O}(\lambda^6)\,. \tag{3.26}$$

Starting with the LP soft function term in (3.20), contributions to the NLP cross section come from expanding the kinematic factors. Focusing on this LP soft function term and recalling the simplification of the D coefficients for this case noted after (3.22), we start from

$$\Delta^{\rm kin}_{\rm NLP}(z) = \; H(\hat{s})\,\frac{1}{z}\,\frac{Q}{4\pi}\int \frac{d^{d-1}\vec{q}}{(2\pi)^{d-1}} \int d^d x\, e^{i(\Omega_*/2)x^0 - i(\vec{q}^{\,2}/(2Q))x^0 - i\vec{q}\cdot\vec{x}}\;\widetilde{S}_0\,(x)\,, \tag{3.27}$$

where $H(\hat{s}) = |C^{A0,A0}(x_a n_+ p_A, x_b n_- p_B)|^2$. In the above equation a number of kinematic corrections can be identified. The first is due to power suppression provided by second term in the exponent. The second, originates in the expansion of Ω_* itself. The expansion of the $1/z$ factor gives the third kinematic correction, and a fourth kinematic correction comes from expansion of the argument of the hard function $H(\hat{s})$. After expanding out these terms, the integral over $\vec{q}$ can be performed, yielding a delta function, which sets $\vec{x} = 0$ in the soft function. We write the four corrections in order as

$$\Delta^{K1}_{\rm NLP}(\Omega) = H\big(Q^2\big)\,\frac{\partial}{\partial\Omega}\,\partial^2_{\vec{x}}\,S_{\rm DY}(\Omega,\vec{x})|_{\vec{x}=0}\,, \tag{3.28}$$

$$\Delta^{K2}_{\rm NLP}(\Omega) = H\big(Q^2\big)\,\frac{3}{4}\,\Omega^2\,\frac{\partial}{\partial\Omega} S_{\rm DY}(\Omega,\vec{x})|_{\vec{x}=0}\,, \tag{3.29}$$

$$\Delta^{K3}_{\rm NLP}(\Omega) = H\big(Q^2\big)\;\Omega\,S_{\rm DY}(\Omega,\vec{x})|_{\vec{x}=0}\,, \tag{3.30}$$

$$\Delta^{K4}_{\rm NLP}(\Omega) = H'\big(Q^2\big)\,Q^2\,\Omega\,S_{\rm DY}(\Omega,\vec{x})|_{\vec{x}=0}, \tag{3.31}$$

where $S_{\rm DY}(\Omega,\vec{x}\,)$ is the LP soft function defined in (2.12), but with argument x^0 generalized to non-zero $\vec{x}$. The full NLP kinematic correction, $\Delta^{\rm kin}_{\rm NLP}(z)$, is given by the sum of these four terms. In section 5 we present the result of evaluating these expressions up to NNLO.

JHEP07(2020)078

3.2.2 Dynamical NLP power correction $\Delta^{\rm dyn}_{\rm NLP}(z)$

Next we consider the contribution to the NLP cross section due to insertions of subleading-power Lagrangians and LP kinematics. Thus we keep only the first term in the expansions (3.25), (3.26). The $d^{d-1}\vec{q}$ integral then gives a delta function for the spatial part of x, hence in the soft functions we can immediately set $\vec{x}=0$.

As opposed to the kinematic correction, the collinear functions appearing here are non-trivial. Note that the collinear functions will carry the same indices as the corresponding soft function. On top of the indices connecting to the soft function, the collinear functions carry two Dirac and two colour indices, $\gamma\beta$ and fb, from the threshold-collinear and c-PDF fields in the matching equation (3.23). It is understood that the collinear functions, J_i, in (3.20) carry indices as prescribed by (3.23). For instance, the first soft structure in the set (2.25) has one $\mathcal{B}^+$ field and therefore carries an adjoint index A connecting to the collinear function. This means that J_1 carries one additional adjoint index corresponding to the colour generator. Explicitly, $J_1\left(n_+p, x_a n_+p_A;\omega\right)$ in (3.22) stands for $J^A_{1;\gamma\beta,fb}\left(n_+p, x_a n_+p_A;\omega\right)$.

In order to simplify the $\Delta^{\rm dyn}_{\rm NLP}(z)$ part of the factorization formula (3.20) further, we decompose the collinear functions into all possible colour and spinor structures. Continuing with the example from above, this particular collinear function must be proportional to $\mathbf{T}^A_{fb}$ since this is the only structure which carries one adjoint, A, and two fundamental, fb, colour indices. At this point we can define a scalar collinear function multiplied by $\mathbf{T}^A_{fb}$ and move the colour factor into the soft function where it forms part of the trace over the colour indices. In a similar way, the colour factors in other collinear functions can be absorbed into their corresponding soft functions. The dynamical NLP part of (3.20) can then be simplified to

$$\begin{aligned}\Delta^{\rm dyn}_{\rm NLP}(z) = &-\frac{2}{(1-\epsilon)}\,Q\left[\left(\frac{\not{n}_-}{4}\right)\gamma_{\perp\rho}\left(\frac{\not{n}_+}{4}\right)\gamma^\rho_\perp\right]_{\beta\gamma}\\ &\times\int d(n_+p)\,C^{\,A0,A0}\left(n_+p, x_b n_-p_B\right)C^{*A0,A0}\left(x_a n_+p_A,\, x_b n_-p_B\right)\\ &\times\sum_{i=1}^{5}\int\{d\omega_j\}\,J_{i,\gamma\beta}\left(n_+p, x_a n_+p_A;\{\omega_j\}\right)\,S_i(\Omega;\{\omega_j\})+\text{h.c.}\,,\end{aligned}\tag{3.32}$$

where here $\Omega = Q(1-z)$. As in (3.20), the double-valued set $\{\omega_j\}=\{\omega_1,\omega_2\}$, is only required for terms $i=4,5$. For $i=5$, in addition to the Dirac indices $\beta\gamma$ written explicitly, J_i and S_i contain further indices, see the definition of S_5 below, which are contracted among them. As mentioned above, a factor of 2 in this formula comes from the $\bar{c}$-terms. Furthermore, one of the D coefficients always reduces to the LP expression, since at NLP there is no $\mathcal{O}(\lambda)$ amplitude in the $q\bar{q}$-channel, as discussed above. We point out again the main difference to the LP factorization formula, namely the presence of the convolution of a jet function with multi-local, generalized soft functions.[7]

[7]This structure bears resemblance to the SCET treatment of $1/m_b$ suppressed power corrections to semi-leptonic B decay in the so-called shape function region [33, 38, 39].

JHEP07(2020)078

We define the multi-local, generalized soft functions in momentum space as the Fourier transforms

$$S_i(\Omega;\{\omega_j\}) = \int \frac{dx^0}{4\pi}\, e^{i\Omega\, x^0/2} \int \left\{\frac{dz_{j-}}{2\pi}\right\} e^{-i\omega_j z_{j-}}\, S_i(x_0;\{z_{j-}\})\,. \tag{3.33}$$

The position-space soft functions appearing at NLP are given by

$$S_1(x^0;z_-) = \frac{1}{N_c}\,\mathrm{Tr}\langle 0|\bar{\mathbf{T}}\left[Y_+^\dagger(x^0)Y_-(x^0)\right]\mathbf{T}\left(\left[Y_-^\dagger(0)Y_+(0)\right]\frac{i\partial_\perp^\nu}{in_-\partial}\mathcal{B}_{\nu_\perp}^+(z_-)\right)|0\rangle\,, \tag{3.34}$$

$$\begin{aligned} S_{2;\mu\nu}(x^0;z_-) = &\frac{1}{N_c}\,\mathrm{Tr}\,\langle 0|\bar{\mathbf{T}}\left[Y_+^\dagger(x^0)Y_-(x^0)\right] \\ &\times \mathbf{T}\left(\left[Y_-^\dagger(0)Y_+(0)\right]\frac{1}{(in_-\partial)}\left[\mathcal{B}_{\mu_\perp}^+(z_-),\mathcal{B}_{\nu_\perp}^+(z_-)\right]\right)|0\rangle\,, \end{aligned} \tag{3.35}$$

$$\begin{aligned} S_3(x^0;z_-) = &\frac{1}{N_c}\,\mathrm{Tr}\,\langle 0|\bar{\mathbf{T}}\left[Y_+^\dagger(x^0)Y_-(x^0)\right] \\ &\times \mathbf{T}\left(\left[Y_-^\dagger(0)Y_+(0)\right]\frac{1}{(in_-\partial)^2}\left[\mathcal{B}^{+\,\mu_\perp}(z_-),\left[in_-\partial\mathcal{B}_{\mu_\perp}^+(z_-)\right]\right]\right)|0\rangle\,, \end{aligned} \tag{3.36}$$

$$\begin{aligned} S_{4;\mu\nu,bf}^{AB}(x^0;z_{1-},z_{2-}) = &\frac{1}{N_c}\,\mathrm{Tr}\,\langle 0|\bar{\mathbf{T}}\left[Y_+^\dagger(x^0)Y_-(x^0)\right]_{ba} \\ &\times \mathbf{T}\left(\left[Y_-^\dagger(0)Y_+(0)\right]_{af}\mathcal{B}_{\mu_\perp}^{+A}(z_{1-})\mathcal{B}_{\nu_\perp}^{+B}(z_{2-})\right)|0\rangle\,, \end{aligned} \tag{3.37}$$

$$\begin{aligned} S_{5;bfgh,\sigma\lambda}(x^0;z_{1-},z_{2-}) = &\frac{1}{N_c}\,\langle 0|\bar{\mathbf{T}}\left[Y_+^\dagger(x^0)Y_-(x^0)\right]_{ba} \\ &\times \mathbf{T}\left(\left[Y_-^\dagger(0)Y_+(0)\right]_{af}\frac{g_s^2}{(in_-\partial_{z_1})(in_-\partial_{z_2})}q_{+\sigma g}(z_{1-})\bar{q}_{+\lambda h}(z_{2-})\right)|0\rangle\,. \end{aligned} \tag{3.38}$$

We recall from the discussion of the list (2.25) that the soft functions S_2 and S_3 are redundant and could be eliminated by relating them to S_4. There exists in principle another soft function,

$$\begin{aligned} \widetilde{S}_{6;bf,\mu\nu}^A(x;\omega) = &\int dz_-\, e^{-i\omega\, z_-}\frac{1}{N_c}\langle 0|\bar{\mathbf{T}}\left[Y_+^\dagger(x)Y_-(x)\right]_{ba} \\ &\times \mathbf{T}\left(\left[Y_-^\dagger(0)Y_+(0)\right]_{af}\frac{i\partial_{[\mu_\perp}}{in_-\partial}\mathcal{B}_{\nu_\perp]}^{+A}(z_-)\right)|0\rangle\,, \end{aligned} \tag{3.39}$$

with the soft structure given by the second term in (2.25). This soft function is required to obtain the NLP one-soft-gluon emission amplitude, see appendix B, but does not contribute to the DY cross section at any order in perturbation theory. This is because the soft functions are vacuum matrix elements of Wilson lines and soft field insertions, hence, the only structure which can carry the Lorentz indices of the anti-symmetric structure $\frac{\partial_{[\mu_\perp}}{in_-\partial}\mathcal{B}_{\nu_\perp]}^{+A}(z_-)$ in $\widetilde{S}_{6;bf,\mu\nu}^A(x;\omega)$ is the epsilon tensor. However, this is excluded in QCD by

JHEP07(2020)078

parity conservation. Therefore, only the five soft functions given in (3.34) to (3.38) and their corresponding collinear functions appear in the factorization formula.

The above all-order formulation of NLP threshold factorization and the operator definition of the appearing jet and soft functions is one of the main results of this paper.

3.3 Expansion up to NNLO

In section 5 we will check the NLP factorization formula by comparing to existing fixed-order $\mathcal{O}(\alpha_s^2)$ results in the literature and to own expansion-by-region calculations. To prepare this discussion we consider here the terms that arise in the NNLO expansion of (3.32).

Each of the objects in the formula, the hard matching coefficient $C^{A0,A0}(n_+p, n_-\bar{p})$, the collinear functions $J_i\,(n_+p, x_a\, n_+p_A; \{\omega_j\})$, the soft functions $\widetilde{S}_i(x; \{\omega_j\})$, has a perturbative expansion in the strong coupling. Since at NLP the generalized soft functions contain explicit soft field insertions, as opposed to simply being composed of Wilson lines as at LP, the lowest order at which they can contribute is α_s^1. The hard and the collinear functions can have tree-level contributions. This means that in order to reproduce NLO results, only one combination is needed, tree-level hard and collinear functions and a NLO soft function. Then, to reproduce the NNLO fixed order results, there are three contributions: (1) Tree-level hard function together with one-loop collinear and soft functions, (2) one-loop hard function, tree-level collinear and one-loop soft function, and finally, (3) the soft functions at $\mathcal{O}(\alpha_s^2)$.

Before proceeding, it is important to note that since the kinematic set-up allows only for soft radiation, the large component of the incoming PDF-collinear momentum must be identical to the sum of the large components of the outgoing threshold momenta of the collinear function. Since for the A0 current there is only one outgoing momentum, the collinear functions relevant to NLP will be be proportional to $\delta(n_+p - x_a n_+p_A)$. However, due to the presence of n_-z in the soft-collinear interactions, which translates into a n_+p derivative in momentum space, the momentum-space collinear functions can also contain derivatives of the momentum-conserving delta function. This occurs for $J_1(n_+p, x_a\, n_+p_A; \omega)$. Since it is also diagonal in the Dirac indices we write this collinear function in terms of two scalar components as follows:

$$J_{1;\gamma\beta}\,(n_+p, x_a\, n_+p_A; \omega) = \delta_{\gamma\beta}\,\Big[J_{1,1}\,(x_a n_+p_A; \omega)\,\delta(n_+p - x_a n_+p_A) + J_{1,2}\,(x_a n_+p_A; \omega)\,\frac{\partial}{\partial(n_+p)}\delta(n_+p - x_a n_+p_A)\Big]\,. \tag{3.40}$$

In the factorization formula, we can integrate by parts the derivative such that it acts on the amplitude hard-scattering coefficient. Hence the derivative collinear-function term contributes only when the hard matching coefficient is momentum-dependent, which happens only from the one-loop order on for $C^{A0,A0}$. Once the derivative on the coefficient function is taken, one can perform the remaining $d(n_+p)$ integral using the extracted delta function.

The only soft function from the list in (3.34)–(3.38) which begins at lowest, next-to-leading order is S_1. The others contain at least two insertions of subleading soft fields, which

JHEP07(2020)078

implies that the leading contribution to the cross section is NNLO. Therefore, expanded up to NLO, we have

$$\Delta_{\rm NLP}^{\rm dyn\,(1)}(z) = 4Q\,H^{(0)}(Q^2)\int d\omega\,J_{1,1}^{(0)}\,(x_a n_+ p_A;\omega)\,S_1^{(1)}(\Omega;\omega)\,, \tag{3.41}$$

where we have evaluated spin trace, $\mathrm{Tr}\left[\left(\frac{\not n_-}{4}\right)\gamma_{\perp\rho}\left(\frac{\not n_+}{4}\right)\gamma_\perp^\rho\right]$, which gives a factor of $-(1-\epsilon)$. Also, here and below in this section, Ω is related to the threshold variable $1-z$ by $\Omega = Q(1-z)$. Eq. (3.41) can be simplified greatly by inserting the tree-level hard coefficient $H^{(0)}(Q^2) = 1$, and the tree-level collinear function, which can be found in (4.18):

$$\Delta_{\rm NLP}^{\rm dyn\,(1)}(z) = -4\int d\omega\,S_1^{(1)}(\Omega;\omega)\,. \tag{3.42}$$

Moving on to NNLO accuracy, the three contributions discussed above take the following expressions:

- Collinear: one-loop collinear and NLO soft functions

$$\Delta_{\rm NLP-coll}^{\rm dyn\,(2)}(z) = 4Q\,H^{(0)}\big(Q^2\big)\int d\omega\,J_{1,1}^{(1)}\,(x_a n_+ p_A;\omega)\;S_1^{(1)}(\Omega;\omega)\,. \tag{3.43}$$

- Hard: one-loop hard and NLO soft functions

$$\begin{aligned}\Delta_{\rm NLP-hard}^{\rm dyn\,(2)}(z) = 2Q\int d\omega\,S_1^{(1)}\,(\Omega;\omega\,)\,\Bigg(&H^{(1)}\big(Q^2\big)\,J_{1,1}^{(0)}\,(x_a n_+ p_A;\omega)\\ &-C^{*A0\,(0)}\,(x_a n_+ p_A,\,x_b n_- p_B)\,J_{1,2}^{(0)}\,(x_a n_+ p_A;\omega)\\ &\times\frac{\partial}{\partial x_a(n_+p_A)}C^{A0\,(1)}(x_a n_+ p_A, x_b n_- p_B)\Bigg) + \text{h.c.}\end{aligned} \tag{3.44}$$

- Soft: NNLO soft functions

$$\begin{aligned}\Delta_{\rm NLP-soft}^{\rm dyn\,(2)}(z) = &-\frac{4}{(1-\epsilon)}\,Q\left[\left(\frac{\not n_-}{4}\right)\gamma_{\perp\rho}\left(\frac{\not n_+}{4}\right)\gamma_\perp^\rho\right]_{\beta\gamma}H^{(0)}\big(Q^2\big)\\ &\times\sum_{i=1}^{5}\int\{d\omega_j\}\;J_{i,\gamma\beta}^{(0)}\,(x_a\,n_+ p_A;\{\omega_j\})\;S_i^{(2)}(\Omega;\{\omega_j\})\,.\end{aligned} \tag{3.45}$$

  In $\Delta_{\rm NLP-soft}^{\rm dyn\,(2)}(z)$ the derivative terms in the collinear functions do not contribute, since the hard function is taken at tree level.

All of the above formulas can be simplified by using tree-level values for the relevant objects. In particular since $H^{(0)}(Q^2) = 1$, we have

$$\Delta_{\rm NLP-coll}^{\rm dyn\,(2)}(z) = 4Q\int d\omega\,J_{1,1}^{(1)}(x_a\,n_+ p_A;\omega)\,S_1^{(1)}(\Omega;\omega) \tag{3.46}$$

for the collinear term. Next, the hard contribution in (3.44) can be simplified using tree-level values for the collinear functions in (4.18) and (4.19). Care has to be taken when

JHEP07(2020)078

dealing with this expression, since it refers to d-dimensional regularized objects. The one-loop d-dimensional hard matching coefficient depends on $Q^2 = x_a x_b n_+ p_A n_- p_B$ only through an overall factor $(-Q^2/\mu^2)^{-\epsilon}$. Performing the derivative therefore gives back the hard matching coefficient multiplied by a factor of $-\epsilon/Q$. Together with the hermitian conjugate term in (3.44), we obtain $-\epsilon/Q \times (C^{*A0(0)} C^{A0(1)} + C^{*A0(1)} C^{A0(0)}) = -\epsilon\, H^{(1)}/Q$ from the derivative term. Then we arrive at

$$\Delta^{\mathrm{dyn}\,(2)}_{\mathrm{NLP-hard}}(z) = -4\,(1-\epsilon)\, H^{(1)}(Q^2) \int d\omega\, S_1^{(1)}\,(\Omega;\,\omega\,)\,. \tag{3.47}$$

The tree-level collinear functions can also be utilized to simplify the soft term, but we do not present it here.

4 Calculation of collinear functions

In this section we present the computation of the collinear functions to one-loop accuracy. The presence of these functions at NLP is one of the main results of this paper, and we will need the one-loop calculation in the subsequent section to verify the NLP factorization formula to NNLO.

The collinear functions are defined through the non-perturbative operator matching equation (3.23). The left-hand side includes the threshold-collinear fields originating from time-ordered products of the LP current with subleading-power Lagrangian terms. We introduce the abbreviation

$$\tilde{\mathcal{T}}_{\gamma f}(t) \equiv i \int d^4 z\, \mathbf{T}\Big[\chi_{c,\gamma f}\,(t n_+)\, \mathcal{L}^{(2)}(z)\Big]\,, \tag{4.1}$$

for the left-hand side of (3.23), and define its Fourier transform by

$$\mathcal{T}_{\gamma f}(n_+ q) = \int dt\, e^{i(n_+ q)\, t}\, \tilde{\mathcal{T}}_{\gamma f}(t)\,. \tag{4.2}$$

The momentum-space matching equation reads

$$\begin{aligned}\mathcal{T}_{\gamma f}(n_+ q) \,=\, 2\pi \sum_i \int \frac{dn_+ p_a}{2\pi} \int du\, e^{i\,(n_+ p_a)\, u} \int \frac{d\omega}{2\pi} \\ \times\, J_{i;\gamma\beta,\mu,fbd}\,(n_+ q, n_+ p_a; \omega)\; \chi^{\mathrm{PDF}}_{c,\beta b}\,(u n_+) \int dz_-\, e^{-i\omega z_-}\, \mathfrak{s}_{i;\mu,d}(z_-)\,.\end{aligned} \tag{4.3}$$

For soft structures with two soft gluon emissions the generalization explained below (3.23) applies.

We recall that since the collinear scale $Q^2(1-z) \gg \Lambda^2$ by assumption, the collinear function is a perturbatively calculable short-distance coefficient in the matching of (4.1) and (4.3). We can therefore extract the collinear functions J_i by taking an appropriate matrix element between partonic states. For example, in case of collinear functions with a single external soft gluon, the simplest choice is the matrix element $\langle g(k)| \ldots |q(p)\rangle$ with a soft gluon and PDF-collinear quark. We then compute both sides of the matching equation with the LP collinear Lagrangian with soft fields decoupled, in which case the soft fields on both sides act only as external fields. Hence, the soft matrix element $\langle g(k)|\mathfrak{s}_{i;\mu,d}(z_-)|0\rangle$ takes its tree-level expression (since only soft loops could contribute). The same is true for $\langle 0|\chi^{\mathrm{PDF}}_{c,\beta b}(u n_+)|q(p)\rangle$, because loop corrections are scaleless in this case.

JHEP07(2020)078

4.1 Collinear functions at $\mathcal{O}(\alpha_s^0)$

For the $q\bar{q}$-induced DY process, only the insertions of the quark-gluon subleading SCET Lagrangian but not the Yang-Mills terms contribute at tree level to the collinear functions. Indeed, at least one collinear gluon loop would be needed to which a $\mathcal{L}^{(2)}_{\rm YM}$ insertion could be attached via a triple-gluon interaction.

We use momentum-space Feynman rules for the soft-collinear interactions vertices from the power-suppressed SCET Lagrangian given in appendix A of [35] to perform the computation. The collinear-quark soft-gluon interaction vertex is given by

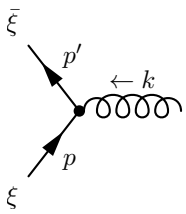

$$ig_s\mathbf{T}^A \begin{cases} \dfrac{\not{n}_+}{2} n_{-\mu} & \mathcal{O}(\lambda^0) \\ \dfrac{\not{n}_+}{2} X_\perp^\rho n_-^\nu (k_\rho g_{\nu\mu} - k_\nu g_{\rho\mu}) & \mathcal{O}(\lambda) \\ S^{\rho\nu}(k,p,p') \dfrac{\not{n}_+}{2} (k_\rho g_{\nu\mu} - k_\nu g_{\rho\mu}) & \mathcal{O}(\lambda^2) \end{cases}$$

where

$$S^{\rho\nu}(k,p,p') \equiv \frac{1}{2}\left[(n_-X)n_+^\rho n_-^\nu + (kX_\perp)X_\perp^\rho n_-^\nu + X_\perp^\rho \left(\frac{\not{p}'_\perp}{n_+p'}\gamma_\perp^\nu + \gamma_\perp^\nu \frac{\not{p}_\perp}{n_+p}\right)\right] \tag{4.4}$$

and

$$X^\sigma = -\frac{\partial}{\partial p'_\sigma}\left((2\pi)^d \delta^{(d)}(p - p' + k_+)\right) . \tag{4.5}$$

The momentum k_+, which appears in the argument of the delta function above, is defined as $k_+^\mu = (n_-k)\frac{n_+^\mu}{2}$. The three terms in the $\mathcal{O}(\lambda^2)$ vertex (4.4) correspond directly to the three terms in the power-suppressed SCET Lagrangian given in eq. (28) of [29]. This has been rewritten in terms of gauge-invariant building blocks in (A.1) such that the first term in (4.4) corresponds to $\mathcal{L}^{(2)}_{1\xi}$, the second term to $\mathcal{L}^{(2)}_{2\xi}$, and the third term to $\mathcal{L}^{(2)}_{4\xi}$. In appendix A we also provide the soft-quark and Yang-Mills SCET Lagrangian in this notation, which are needed for the one-loop calculation and for soft structures with soft quarks.

An important feature of the NLP Feynman rules is that they contain derivatives of momentum-conservation delta functions at the subleading-power vertices. This is due to the appearance of explicit position-space arguments, x^μ, in the SCET Lagrangian terms owing to multipole expansion [28]. These derivatives must first be integrated by parts to act on the rest of the amplitude *before* imposing momentum conservation.

4.1.1 Single soft gluon structures

Inspection of the subleading-power SCET Lagrangian (A.1) shows that only the two soft gluon structures

$$\mathfrak{s}_1^A(z_-) = \frac{i\partial_\perp^\mu}{in_-\partial}\mathcal{B}_{\mu_\perp}^{+A}(z_-) \qquad \text{and} \qquad \mathfrak{s}_6^A(z_-) = \frac{i\partial_{[\mu_\perp}}{in_-\partial}\mathcal{B}_{\nu_\perp]}^{+A}(z_-) \tag{4.6}$$

JHEP07(2020)078

can have tree-level single-gluon matrix elements at $\mathcal{O}(\lambda^2)$. Hence the sum over i in (4.3) reduces to $i = 1, 6$. Explicitly, (4.3) turns into

$$\begin{aligned}\langle g(k)^K|\mathcal{T}^{1g}_{\gamma f}(n_+q)|q(p)_e\rangle &= 2\pi \int \frac{dn_+p_a}{2\pi} du\, e^{i\,(n_+p_a)\,u} \int \frac{d\omega}{2\pi} \int dz_-\, e^{-i\,\omega\, z_-} \\ &\times \Big(J^A_{1;\gamma\beta,fb}\,(n_+q, n_+p_a;\omega)\,\langle 0|\chi^{\rm PDF}_{c,\beta b}(un_+)|q(p)_e\rangle\langle g(k)^K|\mathfrak{s}^A_1(z_-)\,|0\rangle \\ &+ J^{\mu\nu,A}_{6;\gamma\beta,fb}\,(n_+q, n_+p_a;\omega)\,\langle 0|\chi^{\rm PDF}_{c,\beta b}(un_+)|q(p)_e\rangle\langle g(k)^K|\mathfrak{s}^A_{6;\mu\nu}(z_-)\,|0\rangle\Big)\,,\end{aligned} \tag{4.7}$$

where K, e refer to the colour of the external state and the superscript $1g$ reminds us that we consider the collinear functions for single soft gluon emission.

The c-PDF collinear matrix element on the right-hand side equals

$$\langle 0|\chi^{\rm PDF}_{c,\beta b}(un_+)|q(p)_e\rangle = \delta_{be}\sqrt{Z_{q,\rm PDF}}\, u_{c,\beta}(p)\, e^{-i(n_+p)\,u}\,, \tag{4.8}$$

where $\sqrt{Z_{q,\rm PDF}}$ is the on-shell wave renormalization factor of the c-PDF field. The soft matrix elements are found to give

$$\langle g(k)^K|\frac{i\partial^\nu_\perp}{in_-\partial}\mathcal{B}^{+\,A}_{\nu_\perp}(z_-)\,|0\rangle = \delta^{AK}\,\frac{g_s}{(n_-k)}\left[k^\eta_\perp - \frac{k^2_\perp}{(n_-k)}n^\eta_-\right]\epsilon^*_\eta(k)\,e^{iz_-k}\,, \tag{4.9}$$

$$\langle g(k)^K|\frac{i\partial_{[\mu_\perp}}{in_-\partial}\mathcal{B}^{+\,A}_{\nu_\perp]}(z_-)|0\rangle = \delta^{AK}\,\frac{g_s}{(n_-k)}\left[k^\mu_\perp\, g^{\nu\eta}_\perp - k^\nu_\perp\, g^{\mu\eta}_\perp\right]\epsilon^*_\eta(k)\,e^{iz_-k}\,. \tag{4.10}$$

Inserting these results into (4.7), we obtain

$$\begin{aligned}\langle g(k)^K|\mathcal{T}^{1g}_{\gamma f}(n_+q)|q(p)_e\rangle &= 2\pi\,\frac{g_s}{(n_-k)}\Bigg(J^K_{1;\gamma\beta,fe}\,(n_+q, n_+p; n_-k)\left[k^\eta_\perp - \frac{k^2_\perp}{(n_-k)}n^\eta_-\right] \\ &+ J^{\mu\nu,K}_{6;\gamma\beta,fe}\,(n_+q, n_+p; n_-k)\,\left[k^\mu_\perp\, g^{\nu\eta}_\perp - k^\nu_\perp\, g^{\mu\eta}_\perp\right]\Bigg)\sqrt{Z_{q,\rm PDF}}\, u_{c,\beta}(p)\epsilon^*_\eta(k)\,.\end{aligned} \tag{4.11}$$

This is the final expression for the right-hand side of the matching equation (4.3) for single soft gluon structures for the chosen partonic state. We note that this expression is exact to all orders in perturbation theory, since, as mentioned above, there are no loop corrections to the above matrix elements.

We next turn our attention to the computation of the left-hand side of the matching equation (4.3). The relevant terms in $\mathcal{L}^{(2)}$ are $\mathcal{L}^{(2)}_{1\xi,2\xi,4\xi}$, which give rise to the NLP soft-gluon vertex (4.4). A straightforward tree-level calculation gives

$$\begin{aligned}\langle g(k)^K|\mathcal{T}^{1g}_{\gamma f}(n_+q)|q(p)_e\rangle &= 2\pi\,\frac{g_s}{(n_-k)}\mathbf{T}^K_{fe}\Bigg\{ \\ &- \left[k^\eta_\perp - \frac{k^2_\perp}{(n_-k)}n^\eta_-\right]\frac{1}{n_+p}\delta(n_+q - n_+p)\delta_{\gamma\beta} \\ &- \left[(n_-k)n^\eta_+ - (n_+k)n^\eta_-\right]\frac{\partial}{\partial n_+q}\delta(n_+q - n_+p)\delta_{\gamma\beta} \\ &- \left[k^\mu_\perp g^{\nu\eta}_\perp - k^\nu_\perp g^{\mu\eta}_\perp\right]\frac{1}{2}\frac{1}{n_+p}\delta(n_+q - n_+p)\left[\gamma^\mu_\perp\gamma^\nu_\perp\right]_{\gamma\beta}\Bigg\} \\ &\times \epsilon^*(k)_\eta\,\sqrt{Z_{q,c}}|_{\rm tree}\, u_{c,\beta}(p) + \mathcal{O}(\alpha_s)\,,\end{aligned} \tag{4.12}$$

JHEP07(2020)078

where $\sqrt{Z_{q,c}}|_{\text{tree}} = 1$ is the tree-level value of the on-shell wave function renormalization factor of the quark field in the effective theory including the threshold-collinear mode. Calculating the contribution directly using the Feynman rule (4.4) gives three contributions proportional to different soft structures. However, they are not independent, as they are connected via the equation-of-motion identity (2.26). We can use the transversality and on-shell conditions $k\cdot\epsilon^* = 0$ and $k^2 = 0$, respectively, for the emitted gluon, which have not yet been exploited in obtaining (4.12). The relation $k\cdot\epsilon^* = 0$ can be written in light-cone components as

$$(n_+k)(n_-\epsilon^*) = 2\left(-\frac{(n_-k)(n_+\epsilon^*)}{2} - k_\perp\cdot\epsilon^*_\perp\right), \tag{4.13}$$

at which point we see that indeed we can express the second soft structure in the curly bracket of (4.12) in terms of the first,

$$\left[(n_-k)n_+^\nu - (n_+k)n_-^\nu\right]\epsilon^*_\nu(k) = -2\left[k_\perp^\nu - \frac{k_\perp^2}{(n_-k)}n_-^\nu\right]\epsilon^*_\nu(k)\,. \tag{4.14}$$

This is expected as we know that the insertions of $\mathcal{L}^{(2)}_{1\xi}$ and $\mathcal{L}^{(2)}_{2\xi}$ contribute to the same collinear function J_1, since the soft structures are connected via (2.26). Using this relation, we arrive at

$$\begin{aligned}\langle g(k)^K|\mathcal{T}^{1g}_{\gamma f}(n_+q)|q(p)_e\rangle = 2\pi\,\frac{g_s}{(n_-k)}\mathbf{T}^K_{fe}\Bigg\{&\\ \left[k_\perp^\eta - \frac{k_\perp^2}{(n_-k)}n_-^\eta\right]&\left(-\frac{1}{n_+p}\delta(n_+q-n_+p) + 2\,\frac{\partial}{\partial n_+q}\delta(n_+q-n_+p)\right)\delta_{\gamma\beta}\\ -\left[k_\perp^\mu g_\perp^{\nu\eta} - k_\perp^\nu g_\perp^{\mu\eta}\right]&\frac{1}{2}\frac{1}{n_+p}\delta(n_+q-n_+p)\left[\gamma_\perp^\mu\gamma_\perp^\nu\right]_{\gamma\beta}\Bigg\}\\ \times\,\epsilon^*(k)_\eta\,\sqrt{Z_{q,c}}|_{\text{tree}}\,u_{c,\beta}(p) + \mathcal{O}(\alpha_s)\,.&\end{aligned} \tag{4.15}$$

Through comparison of (4.15) to (4.11), we find the tree-level collinear functions

$$J^{K(0)}_{1;\gamma\beta,fe}(n_+q,n_+p;\omega) = \mathbf{T}^K_{fe}\delta_{\beta\gamma}\left(-\frac{1}{n_+p}\delta(n_+q-n_+p) + 2\,\frac{\partial}{\partial n_+q}\delta(n_+q-n_+p)\right), \tag{4.16}$$

$$J^{\mu\nu,K(0)}_{6;\gamma\beta,fe}(n_+q,n_+p;\omega) = -\frac{1}{2}\frac{1}{n_+p}\mathbf{T}^K_{fe}\left[\gamma_\perp^\mu\gamma_\perp^\nu\right]_{\gamma\beta}\delta(n_+q-n_+p)\,. \tag{4.17}$$

We would like to draw attention to the factor of -2 in the second term of (4.16) relative to the first that was not present in (4.12). Its origin can be traced back to the fact that the soft fields in the two terms giving rise to this contribution are connected by the equation-of-motion relation (2.26) precisely with this weight. For the decomposition of the scalar collinear function J_1 introduced in (3.40), eq. (4.16) implies

$$J^{(0)}_{1,1}(n_+p;\omega) = -\frac{1}{n_+p}\,, \tag{4.18}$$

$$J^{(0)}_{1,2}(n_+p;\omega) = 2\,. \tag{4.19}$$

We recall from section 3.2.2 that the collinear function J_6 does not contribute to the DY cross section to any order in perturbation theory.

JHEP07(2020)078

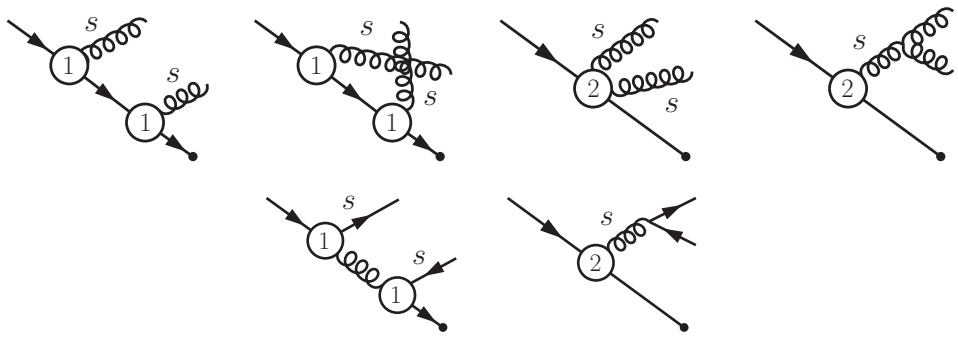

Figure 5. Diagrams contributing to the matching of the two soft parton collinear functions. Soft lines are labelled with an "s". The contributions from the one-soft-particle reducible diagrams, when the internal gluon originates from $n_+\mathcal{B}^+$ term in $\mathcal{L}^{(2)}$, are reproduced by the two parton terms in the equation of motion relation (2.26) applied to (4.12).

4.1.2 Double soft parton structures

We now consider the collinear functions multiplying soft structures with at least two soft fields. In the graphical representation of figure 4, these correspond to diagrams with one external quark to the left and right, and two external soft gluons or a soft quark-antiquark pair attaching to J. The diagrams relevant to the tree-level matching computation are shown in figure 5. Specifically, we require the single insertions of the $\mathcal{L}^{(2)}_{3\xi}$ and $\mathcal{L}^{(2)}_{5\xi}$ Lagrangians, and the double insertions of $\mathcal{L}^{(1)}_{\xi}$ and $\mathcal{L}^{(1)}_{\xi q}$, see appendix A for the definition of these terms. In addition, there exist one-soft-particle-reducible diagrams with an insertion of $\mathcal{L}^{(2)}_{1\xi}$, see the last diagram in each row in figure 5, since we eliminated $n_+\mathcal{B}^+$ from the list of soft structures by the equation-of-motion relation (2.26).

We start with collinear functions associated with two soft gluon emission at the same position z_-. The collinear functions due to insertions of $\mathcal{L}^{(2)}_{3\xi}$ and $\mathcal{L}^{(2)}_{5\xi}$ are calculated as for the single gluon emission, with a generalization of (4.7) to the two-parton case and the $\mathfrak{s}_i$ structures given by third and fourth terms in (2.25). Since both terms involve $\mathcal{B}^+_{\mu_\perp}$ only, we choose the external soft gluon polarizations to be $\perp$ to extract the collinear function. The left-hand side of the matching equation is obtained by calculation of the third diagram in figure 5 with the appropriate Lagrangian insertions. The collinear function J_3, as defined by (3.32) with soft function (3.36), is given by

$$J_{3;\gamma\beta}\left(n_+p, x_a\, n_+p_A;\omega\right) = \delta_{\gamma\beta}\left[J_{3,1}\left(x_a n_+p_A;\omega\right)\delta(n_+p - x_a n_+p_A)\right.$$
$$\left. + J_{3,2}\left(x_a n_+p_A;\omega\right)\frac{\partial}{\partial(n_+p)}\delta(n_+p - x_a n_+p_A)\right] \qquad (4.20)$$

with $J_{3,1}$ and $J_{3,2}$ to be determined. A closer inspection of the subleading-power SCET Lagrangian (A.1) shows that after the soft fields are stripped off, the remaining collinear parts of $\mathcal{L}^{(2)}_{3\xi}$ and $\mathcal{L}^{(2)}_{5\xi}$ are identical to those of $\mathcal{L}^{(2)}_{2\xi}$ and $\mathcal{L}^{(2)}_{4\xi}$, respectively. This means that the collinear functions are the same, that is $J_{3,1}$ is equal to $J_{1,1}$, and J_2 to J_6. The one-soft-particle reducible diagram is only partly reproduced by the already determined

JHEP07(2020)078

single-gluon emission collinear function, since the $n_+\mathcal{B}^+$ soft field was eliminated from the basis of soft structures. The unaccounted piece in this diagram can be determined by explicit matching, or by making use of the single-gluon matrix element (4.12) before the on-shell and transversality of the external soft gluon was enforced. Replacing n_+^η by the operator $n_+\mathcal{B}^+$, and then employing the operator equation-of-motion identity (2.26) results in a term proportional to the two-soft gluon structure $\mathfrak{s}_3$. In this way, we deduce that $J_{3,2}$ in (4.20) is equal to $J_{1,2}$. Alternatively, we could use (2.26) directly in $\mathcal{L}^{(2)}_{1\xi}$, which then contains the same soft-gluon structure as $\mathcal{L}^{(2)}_{3\xi}$, and derive $J_{3,2}$ from the newly generated $q\bar{q}gg$ vertex.

It remains to consider the contribution from the double $\mathcal{L}^{(1)}$ insertions. The collinear matching equation for double Lagrangian insertions is

$$\begin{aligned} i^2 \int d^4z_1\, d^4z_2\, \mathbf{T}\Big[\chi_{c,\gamma f}\,(tn_+)\;\mathcal{L}^{(1)}(z_1)\mathcal{L}^{(1)}(z_2)\Big] &= 2\pi \sum_i \int \frac{dn_+p_a}{2\pi} du\, e^{i\,(n_+p_a)u} \\ &\times \int \frac{d\omega_1}{2\pi}\, dz_{1-}\, e^{-i\omega_1\, z_{1-}} \int \frac{d\omega_2}{2\pi}\, dz_{2-}\, e^{-i\omega_2\, z_{2-}} \int \frac{dn_+p}{2\pi} e^{-i\,(n_+p)t} \\ &\times J_{i;\gamma\beta,\mu,fbd}\,(n_+p, n_+p_a; \omega_1, \omega_2)\, \chi^{\rm PDF}_{c,\beta b}\,(un_+)\, \mathfrak{s}_{i;\mu,d}(z_{1-}, z_{2-})\,. \end{aligned} \tag{4.21}$$

The partonic matrix elements to be calculated here is $\langle g(k_1)g(k_2)|\ldots|q(p)\rangle$. The right-hand side of the matching equation is then obtained as

$$\begin{aligned} \langle g(k_1)^{K_1} g(k_2)^{K_2}|\mathcal{T}^{2g}_{\gamma f}(n_+q)|q(p)_e\rangle &= 2\pi \int \frac{dn_+p_a}{2\pi} du\, e^{i\,(n_+p_a)u} \int \frac{d\omega_1}{2\pi}\, dz_{1-}\, e^{-i\omega_1 z_{1-}} \\ &\times \int \frac{d\omega_2}{2\pi}\, dz_{2-}\, e^{-i\omega_2 z_{2-}} \Big(J^{\mu\nu,AB}_{4;\gamma\beta,fb}\,(n_+q, n_+p_a; \omega_1, \omega_2) \\ &\times \langle 0|\chi^{\rm PDF}_{c,\beta b}(un_+)|q(p)_e\rangle\, \langle g(k_1)^{K_1} g(k_2)^{K_2}|\mathfrak{s}^{AB}_{4;\mu\nu}(z_{1-}, z_{2-})\,|0\rangle\Big)\,, \end{aligned} \tag{4.22}$$

The left-hand side is calculated as for the single soft gluon case, with $\mathcal{L}^{(1)}_\xi$ in (4.21). The relevant diagrams are the first two in the first line of figure 5. After matching both sides of the equation we find

$$\begin{aligned} J^{\mu\nu,AB\,(0)}_{4;\gamma\beta,fb}\,(n_+q, n_+p; \omega_1, \omega_2) &= \frac{2g_\perp^{\mu\nu}}{n_+p\,(\omega_1+\omega_2)^2}\,\big(\,\omega_1\,\mathbf{T}^A\mathbf{T}^B + \omega_2\,\mathbf{T}^B\mathbf{T}^A\,\big)_{fb} \\ &\times \delta_{\gamma\beta}\,\delta(n_+q - n_+p)\,. \end{aligned} \tag{4.23}$$

The calculation of the tree-level soft quark-anti-quark collinear function proceeds in the same way. The double $\mathcal{L}^{(1)}_{\xi q}$ Lagrangian insertion contribution to the partonic matrix element $\langle q(k_1)_{k_1}\bar{q}(k_2)_{k_2}|\ldots|q(p)\rangle$ can be written as

$$\begin{aligned} \langle q(k_1)_{k_1}\bar{q}(k_2)_{k_2}|\mathcal{T}^{2q}_{\gamma f}(n_+q)|q(p)_e\rangle &= 2\pi \int \frac{dn_+p_a}{2\pi} du\, e^{i\,(n_+p_a)u} \int \frac{d\omega_1}{2\pi}\, dz_{1-}\, e^{-i\omega_1 z_{1-}} \\ &\times \int \frac{d\omega_2}{2\pi}\, dz_{2-}\, e^{-i\omega_2 z_{2-}} \Big(J^{fghb}_{5;\gamma\sigma\lambda\beta}\,(n_+q, n_+p_a; \omega_1, \omega_2) \\ &\times \langle 0|\chi^{\rm PDF}_{c,\beta b}(un_+)|q(p)_e\rangle\, \langle q(k_1)_{k_1}\bar{q}(k_2)_{k_2}|\mathfrak{s}_{5;\sigma\lambda,gh}(z_{1-}, z_{2-})\,|0\rangle\Big). \end{aligned} \tag{4.24}$$

JHEP07(2020)078

The left-hand side corresponds to the first diagram in the second line of figure 5. Since for the quark-antiquark case we employed a non-redundant soft basis with the single bi-local soft structure $\mathfrak{s}_5$, the one-soft-particle reducible diagram in the same figure also contributes to J_5. The piece not already accounted for by the single-soft emission followed by a purely soft intercation can be obtained as for the two-gluon case from the quark-antiquark term in the operator equation-of-motion identity (2.26). Adding both contributions, we obtain

$$J^{fk_1k_2e\,(0)}_{5;\gamma\sigma\lambda\beta}(n_+q,n_+p;\omega_1,\omega_2) = -\mathbf{T}^A_{fk_2}\mathbf{T}^A_{k_1e}\,\frac{1}{n_+p}\frac{\omega_2}{(\omega_1+\omega_2)}\frac{\not{n}_{-\gamma\eta}}{2}\gamma^\mu_{\perp,\eta\sigma}\gamma_{\perp\mu,\lambda\beta}\,\delta(n_+q-n_+p)$$
$$+\,2\,\mathbf{T}^K_{fe}\mathbf{T}^K_{k_1k_2}\frac{\omega_1\omega_2}{(\omega_1+\omega_2)^2}\not{n}_{-\lambda\sigma}\delta_{\gamma\beta}\,\frac{\partial}{\partial n_+q}\delta(n_+q-n_+p)\,. \quad (4.25)$$

4.2 Collinear functions at $\mathcal{O}(\alpha_s)$

In this section we focus on demonstrating the consistency of the concept of collinear functions by calculating J_1 and J_6 at the one-loop level. J_1 is also the only collinear function which is needed at the one-loop order to verify the NLP factorization formula at NNLO accuracy, see (3.46). We do not calculate the loop correction to the collinear functions of the two soft-parton structures, since it is a next-to-next-to-next-to-leading order (NNNLO) effect.

The right-hand side of the matching equation has already been obtained in (4.11), which is valid to all orders in α_s. The on-shell wave function renormalization factor should now be evaluated with one-loop accuracy. However, when dimensional regularization is used for ultraviolet and infrared divergences, $\sqrt{Z_{q,\mathrm{PDF}}}=1$ to all orders, because the loops are scaleless.[8] The coupling renormalization is also the same on both sides of the matching equation, and drops out at the one-loop order.

We therefore focus on the calculation of $\langle g(k)^K|\mathcal{T}^{1g}_{\gamma f}(n_+q)|q(p)_e\rangle$ on the left-hand side of (4.3), which requires the calculation of the Feynman diagrams with one collinear loop and a single soft emission, generated by insertions of the power-suppressed Lagrangian. The relevant SCET diagrams are shown in figure 6. The circled vertex denotes the subleading-power Lagrangian insertion, while all other vertices are LP interactions.

4.2.1 Detailed computation

We illustrate the computation by considering as an example the top-left diagram in figure 6, which we draw again with momentum labels in figure 7. All necessary Feynman rules were provided in appendix A of [35] and (4.4). Applying them to the diagram under consideration leads to

$$\langle g(k)^K|\mathcal{T}^{1g}_{\gamma f}(n_+q)|q(p)_e\rangle_{\text{fig. 7}} = -2(2\pi)ig_s^3\left(C_F-\frac{1}{2}C_A\right)\mathbf{T}^K_{fe}\int\frac{d^dp_1}{(2\pi)^d}\int\frac{d^dp_2}{(2\pi)^d} \quad (4.26)$$
$$\times\,\delta(n_+q-n_+p_1-n_+p_2)\,\frac{1}{(n_+p_2)}\,\frac{n_+p_1}{p_1^2}\,\frac{n_+(p-p_2)}{(p-p_2)^2}\,\frac{1}{p_2^2}$$
$$\times\left[S^{\sigma\delta}(-k,p-p_2,p_1)u_c(p)\right]_\gamma\big(-k_\sigma g_{\delta\nu}+k_\delta g_{\sigma\nu}\big)\,\epsilon^{*\nu}(k).$$

[8] The same statement applies to $\sqrt{Z_{q,c}}$ on the left-hand side of the matching equation, which will be used below.

JHEP07(2020)078

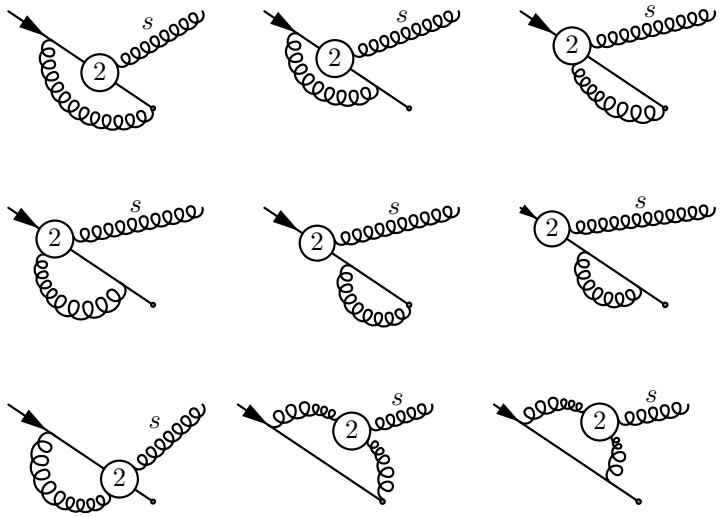

Figure 6. One-loop collinear diagrams with one external soft gluon (labelled "s"). The dot at the right end of the solid quark line denotes the χ_c field from the LP current. The collinear gluon in the loop attaches either to the collinear quark or to the collinear Wilson line in the definition of the χ_c field.

After substituting the expression for $S^{\sigma\delta}(-k, p-p_2, p_1)$ from (4.4) and performing an integration by parts of the derivative with respect to p_1 contained in S, the derivative acts on the integrand including the delta function in the second line. At this point, the momentum conservation delta function at the subleading-power interaction vertex can be imposed by performing the integral over p_1. This identifies $p_1^\mu = p^\mu - p_2^\mu - k_+^\mu$ and results in

$$\begin{aligned}
\langle g(k)^K|\mathcal{T}^{1g}_{\gamma f}(n_+q)|q(p)_e\rangle_{\text{fig. 7}} = &-(2\pi)ig_s^3\left(C_F-\frac{1}{2}C_A\right)\mathbf{T}^K_{fe}\int\frac{d^dp_2}{(2\pi)^d} \\
&\times\frac{1}{(n_+p_2)}\,\frac{n_+(p-p_2)}{(p-p_2)^2}\,\frac{1}{p_2^2}\left(-k_\sigma g_{\delta\nu}+k_\delta g_{\sigma\nu}\right)\epsilon^{*\nu}(k) \\
&\times\Bigg\{n_-\cdot\frac{\partial}{\partial p_1}\left(\delta(n_+q-n_+p_1-n_+p_2)\,\frac{n_+p_1}{p_1^2}\right)n_+^\sigma n_-^\delta\,u_{c,\gamma}(p) \\
&-\left(k_\perp\cdot\frac{\partial}{\partial p_{1\perp}}\right)\frac{\partial}{\partial p_{1\perp\sigma}}\left(\delta(n_+q-n_+p_1-n_+p_2)\frac{n_+p_1}{p_1^2}\right)n_-^\delta\,u_{c,\gamma}(p) \\
&+\frac{\partial}{\partial p_{1\perp\sigma}}\Bigg[\left(\delta(n_+q-n_+p_1-n_+p_2)\,\frac{n_+p_1}{p_1^2}\right) \\
&\times\left(\frac{\not{p}_{1\perp}}{n_+p_1}\gamma_\perp^\delta-\gamma_\perp^\delta\frac{\not{p}_{2\perp}}{n_+(p-p_2)}\right)_{\gamma\beta}\Bigg]u_{c,\beta}(p)\Bigg\}\Bigg|_{p_1=p-p_2-k_+}.
\end{aligned} \tag{4.27}$$

In this equation, only the term with the derivative $n_-\cdot\frac{\partial}{\partial p_1}$ gives a non-vanishing contribution to the derivative component $J_{1,2}$ of the collinear function defined in (3.40), when it acts on the delta function.[9] The remainder of the computation proceeds in the standard

[9]In the factorization formula, once the derivative in (3.40) is integrated by parts, it acts on the hard function, which is, however, constant at tree level. Hence the one-loop correction to $J_{1,2}$ contributes first at NNNLO together with the one-loop hard and soft function.

JHEP07(2020)078

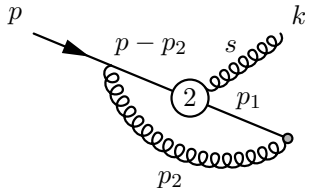

Figure 7. One of the diagrams contributing to the one-loop collinear functions. Through calculation of this diagram using Feynman rules from [35] we can obtain the J_1 and J_6 collinear functions, corresponding to insertions of $\mathcal{L}^{(2)}_{1\xi}$ and $\mathcal{L}^{(2)}_{2\xi}$, and $\mathcal{L}^{(2)}_{4\xi}$, respectively.

way, and we obtain a result valid to all orders in ϵ. Expanding it here for illustration, we find

$$\begin{aligned}\langle g(k)^K|\mathcal{T}^{1g}_{\gamma f}(n_+q)|q(p)_e\rangle_{\text{fig. 7}} = 2\pi\,\frac{g_s\alpha_s}{4\pi}\left(C_F-\frac{1}{2}C_A\right)\frac{\mathbf{T}^K_{fe}}{(n_+p)}\left[\frac{(n_+p)(n_-k)}{\mu^2}\right]^{-\epsilon}\\ \times\Bigg\{\delta(n_+q-n_+p)\Bigg[2\delta_{\gamma\beta}\left(\frac{(n_+k)}{(n_-k)}n^\nu_- - n^\nu_+\right)\\ +\delta_{\gamma\beta}\left(\frac{k^2_\perp\,n^\nu_-}{(n_-k)^2}-\frac{k^\nu_\perp}{(n_-k)}\right)\left(-\frac{2}{\epsilon^2}-\frac{2}{\epsilon}+2+\frac{\pi^2}{6}\right)\\ +\frac{\left[\gamma^\nu_\perp\,,\,\not{k}_\perp\right]_{\gamma\beta}}{(n_-k)}\left(-\frac{1}{\epsilon^2}+\frac{\pi^2}{12}\right)+\mathcal{O}(\epsilon)\Bigg]\\ +\frac{\partial}{\partial n_{+q}}\,\delta(n_+q-n_+p)\,\delta_{\gamma\beta}\left(\frac{(n_+k)}{(n_-k)}n^\nu_- - n^\nu_+\right)\\ \times\left(-\frac{2}{\epsilon^2}-\frac{2}{\epsilon}-4+\frac{\pi^2}{6}+\mathcal{O}(\epsilon)\right)\Bigg\}\,u_{c,\beta}(p)\epsilon^*_\nu(k)\,. \qquad (4.28)\end{aligned}$$

The transversality and on-shell conditions $k\cdot\epsilon^*=0$ and $k^2=0$, respectively, for the emitted gluon, have not yet been used in obtaining (4.28).

4.2.2 Amplitude calculation results

The calculation of all diagrams in figure 6 gives the following result, after using the on-shell and transversality relations:

$$\begin{aligned}&\langle g(k)^K|\mathcal{T}^{1g}_{\gamma f}(n_+q)|q(p)_e\rangle^{(1)}\\ &= 2\pi\,\frac{g_s\alpha_s}{4\pi}\,\mathbf{T}^K_{fe}\left[\frac{k^\eta_\perp}{(n_-k)}-\frac{k^2_\perp n^\eta_-}{(n_-k)^2}\right]\epsilon^*_\eta(k)\,u_{c,\gamma}(p)\,\frac{\delta(n_+q-n_+p)}{n_+p}\left(\frac{n_-k\,n_+p}{\mu^2}\right)^{-\epsilon}\\ &\quad\times\left(C_F\left(-\frac{4}{\epsilon}+3+8\epsilon+\epsilon^2\right)-C_A\left(-5+8\epsilon+\epsilon^2\right)\right)\frac{e^{\epsilon\gamma_E}\,\Gamma[1+\epsilon]\Gamma[1-\epsilon]^2}{(-1+\epsilon)(1+\epsilon)\Gamma[2-2\epsilon]}\\ &\quad+2\pi\,\frac{g_s\alpha_s}{4\pi}\,\mathbf{T}^K_{fe}\left[\frac{k^\mu{}_\perp\epsilon^{*\nu}_\perp(k)}{n_-k}-\frac{k^\nu{}_\perp\epsilon^{*\mu}_\perp(k)}{n_-k}\right]u_{c,\beta}(p)\,\frac{\delta(n_+q-n_+p)}{n_+p}\left(\frac{n_-k\,n_+p}{\mu^2}\right)^{-\epsilon}\\ &\quad\times\left[\gamma^\mu_\perp\gamma^\nu_\perp\right]_{\gamma\beta}(C_F-C_A)\,\frac{e^{\epsilon\gamma_E}\,\Gamma[1+\epsilon]\Gamma[1-\epsilon]^2}{2\,\Gamma[2-2\epsilon]}\,. \qquad (4.29)\end{aligned}$$

JHEP07(2020)078

These results constitute the left-hand side of the matching equation, that is, the extension of (4.15) to one-loop accuracy. Remarkably, we find that the one-loop correction to the derivative delta-function term cancels exactly when all diagrams are added, which explains the absence of such term in the above equation.

4.2.3 Collinear functions results at the one-loop order

Comparing (4.29) to (4.11) we obtain the one-loop correction to J_1 and J_6. We give the d-dimensional result and its expansion in $\epsilon = (4-d)/2$ in the following:

$$J^{K\,(1)}_{1,1;\gamma\beta,fe}(n_+q, n_+p;\,\omega) = \frac{\alpha_s}{4\pi}\delta_{\gamma\beta}\mathbf{T}^K_{fe}\,\frac{1}{(n_+p)}\left(\frac{n_+p\,\omega}{\mu^2}\right)^{-\epsilon}\frac{e^{\epsilon\,\gamma_E}\,\Gamma[1+\epsilon]\Gamma[1-\epsilon]^2}{(-1+\epsilon)(1+\epsilon)\Gamma[2-2\epsilon]} \tag{4.30}$$

$$\times\left(C_F\left(-\frac{4}{\epsilon}+3+8\epsilon+\epsilon^2\right)-C_A\left(-5+8\epsilon+\epsilon^2\right)\right)\delta(n_+q-n_+p)$$

$$= \frac{\alpha_s}{4\pi}\frac{1}{(n_+p)}\,\delta_{\gamma\beta}\mathbf{T}^K_{fe}\left(C_F\left(\frac{4}{\epsilon}+5-4\ln\left(\frac{n_+p\,\omega}{\mu^2}\right)\right)-5C_A\right)\delta(n_+q-n_+p)$$

$$+\,\mathcal{O}(\epsilon)\,, \tag{4.31}$$

$$J^{K\,(1)}_{1,2;\gamma\beta,fe}(n_+q, n_+p;\,\omega) = 0\,, \tag{4.32}$$

$$J^{\mu\nu,\,K\,(1)}_{6;\gamma\beta,fe}(n_+q, n_+p;\,\omega) = \frac{\alpha_s}{4\pi}\frac{1}{(n_+p)}\,\left[\gamma^\mu_\perp\gamma^\nu_\perp\right]_{\gamma\beta}\mathbf{T}^K_{fe}\left(\frac{n_+p\,\omega}{\mu^2}\right)^{-\epsilon}$$

$$\times\frac{e^{\epsilon\,\gamma_E}\,\Gamma[1+\epsilon]\Gamma[1-\epsilon]^2}{2\,\Gamma[2-2\epsilon]}\,(C_F-C_A)\,\delta(n_+q-n_+p) \tag{4.33}$$

$$= \frac{\alpha_s}{4\pi}\frac{1}{2}\frac{1}{(n_+p)}\,\left[\gamma^\mu_\perp\gamma^\nu_\perp\right]_{\gamma\beta}\mathbf{T}^K_{fe}\,(C_F-C_A)\,\delta(n_+q-n_+p)+\mathcal{O}(\epsilon)\,. \tag{4.34}$$

It is noteworthy that there are no $1/\epsilon^2$ poles in the $\mathcal{O}(\alpha_s)$ collinear functions. This implies that there are no leading (double) logarithmic (LL) contributions from the collinear functions and confirms the finding of [14] from the consistency of LL resummation. The absence of the $1/\epsilon^2$ pole results from a cancellation and after applying the equation-of-motion relation, as can be seen from the fact that individual diagrams do contain it, see (4.28). Moreover, for the C_A colour coefficient, even the single pole cancels. The above one-loop corrections to the collinear functions constitute the second main result of this work. As noted earlier, neither $J^{K\,(1)}_{1,2;\gamma\beta,fe}$ nor $J^{K\,(1)}_{6;\gamma\beta,fe}$ contribute to the NNLO DY cross section.

4.2.4 Relation to the LBK ampltiude and the radiative jet function

The study of an amplitude with a next-to-soft emission has a long history starting from the Low-Burnett-Kroll formula and its extension to soft gluon emission from jets [26]. The emergence of the next-to-soft LBK amplitude within SCET was discussed in [40, 41]. The calculation of the collinear functions at the one-loop level presented above forms part of the generalization of the LBK formula to the one-loop order. The complete next-to-soft, one-loop amplitude is provided in appendix B, including terms that vanish at the cross-section level due to the interference with the complex-conjugated tree-level amplitude. The

JHEP07(2020)078

result does not display any suggestive structure, and indeed, to our knowledge there is no simple representation of the one-loop result in terms of the angular momentum operator that would generalize the well-known expression of the tree-level next-to-soft amplitude.

Next-to-soft emission at the one-loop order in amplitudes with a colourless final state has been studied before within the diagrammatic approach [12, 13, 27], where the concept of a "radiative jet function" [26] is used to describe the soft emission from jets. Ultimately, the formalism presented here aims to capture the same physics, however there are conceptual differences. The most important one is that the radiative jet function, as can be found in (2.12) of [13], is not a single scale object unlike the collinear functions defined in (2.23). This fact can be seen in the result for the one-loop radiative jet function given in (3.3) of [13]. In addition to the collinear contributions, there exist subtraction terms which account for the overlap of the radiative jet function with the soft function. No such complications arise here, which makes the effective field theory construction more suitable for resummation using renormalization group techniques. (Nevertheless, NLP resummation near the Drell-Yan threshold using diagrammatic techniques has been achieved at LL accuracy [16] owing to the fact that the radiative jet or collinear functions do not contribute beyond tree level at this accuracy [14].)

Since the radiative jet function contains both collinear and soft contributions, in order to compare our collinear functions with results given in [13] it is necessary to multiply the collinear functions with their corresponding soft structures. At this point, it is most convenient to compare the radiative jet function in [12, 13] with our results for the soft emission amplitude at NLP calculated within SCET and written in appendix B. The relevant contributions are given in (B.4), (B.5), (B.6), and (B.7). We compare these expressions (appropriately expanded in powers of ϵ) with $J^{(1)}_{\mu,F}$ and $J^{(1)}_{\mu,A}$ given in [13]. We find agreement for all terms,[10] except for contributions (B.6) and (B.7) proportional to $n_-^\rho/(n_-l)$. Given that our calculation gives the full amplitude with the emission of a soft gluon, we conclude that the radiative jet function in [12, 13] fails to reproduce the complete amplitude, although the missing terms do not contribute to the matrix element squared at NLP. It would be interesting to investigate further what is the underlying reason for this discrepancy, which is beyond the scope of this work. We speculate that contributions similar to those from the $J^{A0,A1}$ and $J^{A0,B1}$ SCET currents are needed in the radiative jet function formalism.

5 Fixed-order results

There exists a number of NLP results for the DY process at NLO and NNLO in the strong coupling [7, 11–13, 42], obtained from direct expansions of the QCD diagrams. In this section we verify the correctness of the NLP factorization formula by comparing to these results and own results from the expansion-by-regions method [43].

[10] Noting the typo in (3.3) of [13] where one must replace $(-2p\cdot k)^{-\epsilon} \to (2p\cdot k)^{-\epsilon}$ and a overall minus sign error in one-loop results given in [12].

JHEP07(2020)078

5.1 NLO

Expanding the NLP factorization formula to NLO, one finds only one dynamical contribution to the cross section, since the soft function begins at $\mathcal{O}(\alpha_s)$. The one-loop soft function is given by[11]

$$S_1^{(1)}(\Omega,\omega) = \frac{\alpha_s C_F}{2\pi}\frac{\mu^{2\epsilon}e^{\epsilon\gamma_E}}{\Gamma[1-\epsilon]}\frac{1}{\omega^{1+\epsilon}}\frac{1}{(\Omega-\omega)^{\epsilon}}\theta(\omega)\theta(\Omega-\omega)\ . \tag{5.1}$$

Using this result in (3.42) and performing the convolution integral over ω gives

$$\Delta_{\rm NLP}^{\rm dyn\,(1)}(z) = \frac{\alpha_s}{4\pi}C_F\left(\frac{8}{\epsilon} - 16\ln(1-z) - \epsilon\left(2\pi^2 - 16\ln^2(1-z)\right) + O(\epsilon^2)\right), \tag{5.2}$$

where we set $\mu = Q$.

In addition, at NLO we need to take into account the kinematic corrections $\Delta_{\rm NLP}^{K1}(\Omega)$, $\Delta_{\rm NLP}^{K2}(\Omega)$, and $\Delta_{\rm NLP}^{K3}(\Omega)$ in (3.28), (3.29), and (3.30). For the latter two, we can use (5.1) and $H^{(0)}(Q^2) = 1$, since no derivatives with respect to the coordinate $\vec{x}$ needs to be taken. To compute $\Delta_{\rm NLP}^{K1}(\Omega)$ we use the result for the one-loop soft function with full x dependence from [14, 44]. Upon summing the three kinematic corrections we obtain

$$\Delta_{\rm NLP}^{\rm kin\,(1)}(z) = \frac{\alpha_s\, C_F}{4\pi}\Big(8 - \epsilon\, 16\ln(1-z)\Big)\,. \tag{5.3}$$

Results for the NLO NLP contribution to DY production have been presented in [11] within a diagrammatic approach, in which power-suppressed soft radiation is described it terms of generalized next-to-soft Wilson lines. Our result (5.2) agrees with the corresponding expression eq. (6.17) of [11]. The kinematic correction (5.3) is provided in eq. (6.13) of [11] as a correction to the LP matrix element. Agreement can be easily checked. After summing (5.2) and (5.3), and applying the subtractions that arise from PDF renormalization, we also find agreement with the NLO NLP result reported in eq. (B.29) of [42].

5.2 NNLO

In section 3.3 the three possible dynamical NLP contributions to the cross section at NNLO have been discussed. These are collinear, hard, and soft contributions presented in (3.46), (3.47) and (3.45), respectively. In this section we explicitly compute and check the first two of these. The soft contribution requires a full NLP NNLO soft function computation, which is beyond the scope of this work. However, we present the one-virtual, one-real soft contribution to the cross section here. Also, in appendix B we present complete results for the one-loop power-suppressed amplitude with one real soft emission, including the soft loop contribution. The latter forms part of the virtual-real contribution to the NNLO soft function. The missing contribution comes from double real soft emission, which we leave for future work.

[11] The expansion in ϵ was already presented in [14].

JHEP07(2020)078

5.2.1 Collinear contribution

This contribution comes from the one-loop collinear functions combined with the NLO soft function and tree-level hard function, see (3.46). We recall that the delta-function derivative term in the collinear function, spelled out in (3.40), vanishes after partial integration, since the hard function at tree level is a constant. The one-loop collinear function that is required is then given by (4.30) with colour generator and Dirac-index Kronecker-symbol removed.

For the purpose of deriving the NNLO fixed-order result, we keep must use the d-dimensional expression of the collinear function and perform the convolution with the d-dimensional soft function. Then expanding in ϵ and setting $\Omega = Q(1-z)$, $\mu = Q$ yields

$$\begin{aligned}\Delta^{\mathrm{dyn}\,(2)}_{\mathrm{NLP-coll}}(z) = \frac{\alpha_s^2}{(4\pi)^2}\Bigg(C_F^2\Bigg(&-\frac{16}{\epsilon^2}+\frac{48\ln(1-z)-20}{\epsilon}\\ &+\left(-72\ln^2(1-z)+60\ln(1-z)+8\pi^2-24\right)+\mathcal{O}(\epsilon)\Bigg)\\ &+C_A C_F\left(\frac{20}{\epsilon}-(60\ln(1-z)-8)+\mathcal{O}(\epsilon)\right)\Bigg).\end{aligned} \tag{5.4}$$

Notice that, as expected, there are no leading logarithms $\mathcal{O}(\alpha_s^2\ln^3(1-z))$ in the collinear contribution, since the highest power of the logarithm in the finite terms in the second line is NLL accuracy, $\ln^2(1-z)$.

Results describing virtual collinear radiation at one loop with emission of a soft gluon have been derived in [7] within the expansion-by-regions approach [43], and in [12, 13] within a diagrammatic approach, in which the effect of collinear loops is described in terms of a "radiative jet function". The C_F^2 term in (5.4) is in agreement with the corresponding contribution in eqs. (13), (14) of [7] and eq. (4.22) of [12], where the abelian contribution only is considered.[12] The $C_A C_F$ term in our result (5.4) is not provided separately in literature, but only in sum with the hard and soft contribution, that we consider in the following.

5.2.2 Hard contribution

Next we check the contribution composed of the one-loop hard function, the tree-level collinear functions, and the one-loop soft function. In contrast to the collinear contribution, here the collinear function with the derivative contributes, since the hard matching coefficient is momentum-dependent beyond tree level.

The relevant formula is now (3.47), which already made use of the expressions for the collinear functions at tree level. The one-loop soft function was given in (5.1). The d-dimensional hard matching coefficient at the one-loop order can be found in

[12] Notice also that these references drop all contributions proportional to transcendental numbers, such as π^2 and $\zeta(3)$.

JHEP07(2020)078

eq. (2.23) of [45],

$$C^{A0,A0}(n_+p, n_-\bar{p}) = 1 + \frac{\alpha_s}{4\pi} C_F \left(\frac{-Q^2}{\mu^2}\right)^{-\epsilon} \Bigg(-\frac{2}{\epsilon^2} - \frac{3}{\epsilon} - 8 + \frac{\pi^2}{6} + \epsilon \left(\frac{\pi^2}{4} + \frac{14\zeta(3)}{3} - 16\right) + \mathcal{O}(\epsilon^2)\Bigg) + \mathcal{O}(\alpha^2)\,, \tag{5.5}$$

where $Q^2 = (n_+p)(n_-\bar{p})$. Taking care of the imaginary part, the one-loop hard function $H = |C^{A0,A0}|^2$ reads

$$\begin{aligned} H(Q^2) = 1 + \frac{\alpha_s C_F}{4\pi} \Bigg(& -\frac{4}{\epsilon^2} - \frac{1}{\epsilon}\left(4\ln\left(\frac{\mu^2}{Q^2}\right) + 6\right) \\ & - \left(2\ln^2\left(\frac{\mu^2}{Q^2}\right) + 6\ln\left(\frac{\mu^2}{Q^2}\right) - \frac{7\pi^2}{3} + 16\right) + \epsilon\Bigg(-\frac{2}{3}\ln^3\left(\frac{\mu^2}{Q^2}\right) - 3\ln^2\left(\frac{\mu^2}{Q^2}\right) \\ & + \left(\frac{7}{3}\pi^2 - 16\right)\ln\left(\frac{\mu^2}{Q^2}\right) + \frac{28}{3}\zeta(3) + \frac{7}{2}\pi^2 - 32\Bigg) + \mathcal{O}(\epsilon^2)\Bigg) + \mathcal{O}(\alpha_s^2)\,. \end{aligned} \tag{5.6}$$

Performing the ω-integration in (3.47), setting $\mu = Q$, and expanding in ϵ leads to

$$\begin{aligned} \Delta^{\text{dyn}\,(2)}_{\text{NLP}-\text{hard}} = \frac{\alpha_s^2 C_F^2}{(4\pi)^2} \Bigg(& -\frac{32}{\epsilon^3} + \frac{64\ln(1-z) - 16}{\epsilon^2} \\ & + \frac{-64\ln^2(1-z) + 32\ln(1-z) + \frac{80}{3}\left(\pi^2 - 3\right)}{\epsilon} \\ & - \frac{8}{3}\Big(-16\ln^3(1-z) + 12\ln^2(1-z) + 20\left(\pi^2 - 3\right)\ln(1-z) \\ & - 56\zeta(3) - 5\pi^2 + 48\Big) + \mathcal{O}(\epsilon)\Bigg)\,, \end{aligned} \tag{5.7}$$

where $\zeta(3)$ is a Riemann zeta value. In contrast to the NLP collinear contribution, LLs appear in this expression. Resummation of the hard function is therefore necessary in order to sum LLs to all orders in α_s, as was done in [14].

In the literature, the hard one-loop times one real soft gluon result has been considered before within the expansion-by-regions method. The expression for the abelian C_F^2 term has been given in eq. (12) of [7], and agrees with (5.7).[13] Within the diagrammatic approach [12, 13], the hard contribution (5.7) arises from dressing the non-radiative amplitude by a one real soft gluon, according to the LBK theorem. For a discussion of the LBK theorem in the present approach, see [41].

5.2.3 Soft contribution

The soft contribution provided here is the one-real, one-virtual piece of the full NNLO soft function as mentioned in the introduction of section 5.2. In (3.45) one can see that there are contributions to the NNLO soft function from different soft structures. However, as detailed in appendix B.3, only one soft structure, S_1, and corresponding tree-level collinear function actually contribute to this piece. Hence the simplified factorization formula is

$$\Delta^{\text{dyn}\,(2)1r1v}_{\text{NLP}-\text{soft}} = 4Q\, H^{(0)}(Q^2) \int d\omega J^{(0)}_{1,1}\left(x_a(n_+p_A);\omega\right) S_1^{(2)1r1v}(\Omega,\omega). \tag{5.8}$$

[13] We note the following typo in [7]: in eq. (12) $\left[1 + 4\log(1-z)\right]/\epsilon^2$ should be $\left[-1 + 4\log(1-z)\right]/\epsilon^2$.

JHEP07(2020)078

The result for one-real, one-virtual contribution to the two-loop soft function reads

$$S_1^{1r1v}(\Omega,\omega) = -4\,\frac{\alpha_s^2}{(4\pi)^2}C_F C_A\left(-\frac{\omega^2(\Omega-\omega)^2}{\mu^4}\right)^{-\epsilon}\frac{1}{\omega} \times \frac{1}{\epsilon^2}\frac{e^{2\epsilon\gamma_E}\,\Gamma[1-\epsilon]^2}{\Gamma[1-2\epsilon]}\Gamma[1+\epsilon]^2\;\theta(\Omega-\omega)\theta(\omega). \tag{5.9}$$

Using (4.18) for the tree-level collinear function in (5.8), integrating over ω and expanding in ϵ yields

$$\Delta^{\text{dyn}\,(2)1r1v}_{\text{NLP}-\text{soft}} = \frac{\alpha_s^2}{(4\pi)^2}C_F C_A\left(-\frac{8}{\epsilon^3}+\frac{32\ln(1-z)}{\epsilon^2}-\frac{64\ln^2(1-z)}{\epsilon}+\frac{28\pi^2}{3\epsilon} +\frac{256}{3}\ln^3(1-z)-\frac{112}{3}\pi^2\ln(1-z)+\frac{448\zeta(3)}{3}+\mathcal{O}(\epsilon)\right). \tag{5.10}$$

In the literature the non-abelian $C_F C_A$ term of the one-real, one-virtual contribution has been provided as a sum of the collinear, soft and kinematic correction (see eq. (4.6) of [13]), thus (5.10) cannot be compared directly. We performed an independent calculation of the full one-real, one-virtual correction within the expansion-by-regions method, and (5.10) agrees with the soft region, as it should be.

5.2.4 Kinematic contribution

The kinematic correction from the sum of terms (3.28)–(3.31) can also be obtained at NNLO by using the NNLO soft function with full x-dependence presented in [44]. We find

$$\Delta^{\text{kin}\,(2)}_{\text{NLP}}(z) = \frac{\alpha_s^2}{(4\pi)^2}\left[C_F^2\left(\frac{16}{\epsilon^2}-\frac{192\ln(1-z)+96}{\epsilon}+512\ln^2(1-z) +192\ln(1-z)-40\pi^2-256\right)+C_F C_A\left(\frac{88}{3\epsilon}-\frac{352\ln(1-z)}{3} -\frac{8\pi^2}{3}+\frac{476}{9}\right)+C_F n_f\left(-\frac{16}{3\epsilon}+\frac{64\ln(1-z)}{3}-\frac{56}{9}\right)\right]. \tag{5.11}$$

We note that there are no LLs due to kinematic corrections.

The kinematic contribution has been calculated previously within the expansion-by-regions or the diagrammatic approach as the NLP phase-space corrections to the LP matrix element, but the expression corresponding to (5.11) has not been provided explicitly. (It is part of eq. (4.6) and (5.2) of [13], but it cannot be separated from the NLP matrix element.) We thus compare (5.11) with an own independent expansion-by-regions calculation, in which we take the matrix element at leading power (both one-real, one-virtual and two-real diagrams), and integrate it against the NLP phase space, finding agreement.

6 Ill-defined convolution

One of the primary uses of factorization formulas in SCET is to perform resummation using renormalization group equations. Soft-collinear factorization often involves convolutions $C\otimes F$ of hard functions with collinear factors, for example, in deep-inelastic scattering

JHEP07(2020)078

or in convolutions with PDFs for any hadronic scattering cross section, or $J \otimes S$ of jet with soft functions, for example in the description of radiation from final-state jets. Resummation relies on defining renormalized factors by subtracting their poles in dimensional regularization and deriving a renormalization group equation for the renormalized function, which usually also has a convolution form. Large logarithms are then summed by evolving one function to the characteristic scale of the other. Finally, the convolution of the two factors is done.

This procedure evidently requires that the final convolution integral of the renormalized factors is well defined. As we discuss now, this important requirement is not satisfied by the NLP factorization formula for the DY process.

The issue is most clearly exposed when we focus on the functional form of the objects appearing in the one-loop collinear times one-loop soft NNLO term in factorization formula given in (3.46). The one-loop collinear function $J^{(1)}_{1,1}$ is taken from (4.30) and the soft function from (5.1). The convolution integral reads

$$\int_0^\Omega d\omega \, \underbrace{\left(n_+ p\, \omega\right)^{-\epsilon}}_{\text{collinear piece}} \underbrace{\frac{1}{\omega^{1+\epsilon}} \frac{1}{(\Omega-\omega)^{\epsilon}}}_{\text{soft piece}} \,. \tag{6.1}$$

It is evident that the integral is well defined when keeping the exact ϵ dependence in the integrand, as was done in the previous section in order to obtain and reproduce the fixed-order NNLO NLP results. However, as explained above, for resummation we would like to treat the parts originating in the collinear function, $(n_+ p\, \omega)^{-\epsilon}$, and the soft function pieces, $\omega^{-1-\epsilon}\,(\Omega-\omega)^{-\epsilon}$, independently. That is, we wish to expand each in ϵ and define renormalized functions. However, it is clear that there is a problem when this procedure is attempted in (6.1). Concretely, one encounters a divergent integral, or $\int d\omega\, \delta(\omega) \ln(\omega)$ and other ill-defined integrals after introducing the standard plus distribution for the $1/\omega^{1+\epsilon}$ factor.[14]

In order to make the issue even more explicit, we take the ϵ-expanded collinear function given in (4.31) and also expand the one-loop soft function (5.1) in ϵ,

$$S_1^{(1)}\left(\Omega,\omega\right) = \frac{\alpha_s C_F}{4\pi}\left(2\,\delta(\omega)\,\theta(\Omega)\left(-\frac{1}{\epsilon}+\ln\left(\Omega^2/\mu^2\right)\right) + 2\left[\frac{1}{\omega}\right]_+ \theta(\omega)\theta(\Omega-\omega)\right). \tag{6.2}$$

The convolution of this expression with (4.31) according to (3.46) (at $\mu = Q$ as in the section above) gives

$$\begin{aligned}\Delta^{\text{dyn}\,(2)}_{\text{NLP}-\text{coll}}(z) = \frac{\alpha_s^2}{(4\pi)^2}\Bigg(C_F^2\left(-\frac{32}{\epsilon^2}-\frac{8}{\epsilon}\left[5-8\ln(1-z)-4\int d\omega\,\delta(\omega)\ln\left(\frac{\omega}{Q}\right)\right]\right) \\ + C_A C_F\,\frac{40}{\epsilon} + \mathcal{O}(\epsilon^0)\Bigg)\end{aligned} \tag{6.3}$$

[14] In principle, one can move integer powers of ω from the collinear to the soft function by adjusting powers of $1/in_-\partial$. However, this does not solve the problem, since there will always be a factor of $\omega^{-n\epsilon}$ associated with the collinear function.

JHEP07(2020)078

where only the pole terms in ϵ are shown. There are two issues with this result. First, one of the terms with $1/\epsilon$ pole is ill-defined as we encounter the integral $\int d\omega\, \delta(\omega) \ln(\omega)$. Second, the coefficient of the C_F^2/ϵ^2, $C_F C_A/\epsilon$ pole terms which are not divergent have changed with respect to the correct result from (5.4) obtained from expanding in ϵ *after* performing the convolution in d dimensions.

It is clear from the above that it is not possible to obtain the NLP logarithms of $(1-z)$ correctly from the standard renormalization procedure and four-dimensional convolutions. The leading logarithms in the $q\bar{q}$ (gg) channels in DY (Higgs) production summed in [14, 15] form an exception, since they require only tree-level collinear functions and since the loop corrections to the collinear functions do not contribute leading logarithms. The ill-defined convolution, however, hampers the extension of resummation to NLL. The convolution itself requires subtraction, and contributes to the logarithms, which can therefore not be obtained from the separate renormalization group equations for the renormalized collinear and soft functions. Nevertheless, the NLP formula derived in this paper factorizes the different momentum scales of the DY process consistently at the level of regularized matrix elements of the soft and collinear operators, and therefore can be justifiably called a factorization formula. It may be hoped that it provides the starting point for understanding how to renormalize d-dimensional convolutions, which appear to be a generic feature of NLP factorization.[15]

7 Summary

In this work, we derived for the first time a factorization formula for DY production near threshold in the $q\bar{q}$-channel at general powers in the $(1-z)$ expansion. We then focused on the next-to-leading power, which entails several simplifications. The main result is the NLP factorization formula (3.32), which generalizes the LL-accurate formula in [14].

As one of the new key ingredients of the subleading-power factorization formula, we identify and discuss the emergence of collinear functions at the amplitude level. While the related concept of a "radiative jet function" [26] has been known to be relevant to power corrections at the DY threshold from diagrammatic studies [12, 13, 27], the benefit of the present SCET treatment is an operator definition, which renders the function gauge-invariant by construction. More precisely, see (2.23), the collinear functions are the perturbative matching coefficients, when threshold-collinear fields are matched to c-PDF fields in the presence of external soft structures that describe the emission of one (or several) soft gluons. Due to the strict scale separation and systematic power expansion, the collinear functions are single-scale objects. They are extracted from partonic matrix elements since the threshold-collinear scale is assumed to be much larger than the scale of strong interactions, $Q(1-z)^{1/2} \gg \Lambda$.

The tree-level collinear function required for LL resummation in threshold DY (and Higgs) production has already been used in [14, 15]. In this work, we computed the one-loop $\mathcal{O}(\alpha_s)$ corrections (4.30) and (4.33) to the collinear functions, which can contribute to the DY cross section at NNLO, and to the one-loop one-gluon emission amplitude. These

[15] See also [36], where a different type of divergent convolution is discussed.

JHEP07(2020)078

results confirm explicitly the observation made in [14, 15] that the DY collinear function cannot contain LLs. The one-loop calculation demonstrates the validity of the definition of these NLP objects and allows us to verify the correctness of the factorization formula at NNLO by comparing its expansion in powers of α_s with existing results obtained at this order with the expansion-by-regions method.

However, our investigation also highlights that factorization at NLP is not yet understood at a similar level as at LP. The factorization formula separates the scales relevant to the DY threshold in the form of well-defined, dimensionally regulated collinear and soft functions, which have to be convoluted in the soft momentum variables ω_i. The $\mathcal{O}(\alpha_s^2)$ calculation makes explicit what can already be seen from general scaling arguments that the convolutions exist only for the d-dimensional functions. When the expansion in ϵ is performed before the convolution, the latter is ill-defined and leads to a divergence. This implies that the formula is not yet in a form suitable for the resummation of large threshold logarithms beyond the LLs through the renormalization group equations for renormalized hard, collinear and soft functions. Nevertheless, it may be hoped that it provides the starting point for understanding how to renormalize d-dimensional convolutions, which would open the path to NLL resummations beyond LP.

Acknowledgments

We thank M. Garny and J. Wang for useful insights and R. Szafron for many fruitful discussions and technical advice. MB, AB and LV thank the Munich Institute for Particle and Astroparticle Physics (MIAPP) for hospitality during the 2017 programme "Automated, Resummed and Effective: Precision Computations for the LHC and Beyond", where some of the concepts of this work have been developed. LV is supported by Fellini - Fellowship for Innovation at INFN, funded by the European Union's Horizon 2020 research programme under the Marie Skłodowska-Curie Cofund Action, grant agreement no. 754496. This work has been supported by the Bundesministerium für Bildung and Forschung (BMBF) grant no. 05H18WOCA1, by the Dutch National Organization for Scientific Research (NWO) and by the ERC Starting Grant REINVENT-714788.

A Subleading SCET Lagrangian

A.1 Quark-gluon subleading SCET Lagrangian

The quark-gluon interaction terms of subleading power in the soft-collinear SCET Lagrangian [29] are given by

$$\begin{aligned}
\mathcal{L}_{\xi}^{(1)} &= \bar{\chi}_c i x_\perp^\mu \left[i n_- \partial \mathcal{B}_\mu^+ \right] \frac{\not{n}_+}{2} \chi_c, \\
\mathcal{L}_{1\xi}^{(2)} &= \frac{1}{2} \bar{\chi}_c i n_- x \, n_+^\mu \left[i n_- \partial \mathcal{B}_\mu^+ \right] \frac{\not{n}_+}{2} \chi_c, \\
\mathcal{L}_{2\xi}^{(2)} &= \frac{1}{2} \bar{\chi}_c x_\perp^\mu x_\perp^\nu \left[i \partial_\nu i n_- \partial \mathcal{B}_\mu^+ \right] \frac{\not{n}_+}{2} \chi_c,
\end{aligned}$$

JHEP07(2020)078

$$
\begin{aligned}
\mathcal{L}^{(2)}_{3\xi} &= \frac{1}{2}\bar{\chi}_c x^\mu_\perp x^\nu_\perp \left[\mathcal{B}^+_\nu, in_-\partial\mathcal{B}^+_\mu\right]\frac{\not{n}_+}{2}\chi_c,\\
\mathcal{L}^{(2)}_{4\xi} &= \frac{1}{2}\bar{\chi}_c\left(i\not{\partial}_\perp + \not{\mathcal{A}}_{c\perp}\right)\frac{1}{in_+\partial} ix^\mu_\perp\gamma^\nu_\perp\left[i\partial_\nu\mathcal{B}^+_\mu - i\partial_\mu\mathcal{B}^+_\nu\right]\frac{\not{n}_+}{2}\chi_c + \text{h.c.},\\
\mathcal{L}^{(2)}_{5\xi} &= \frac{1}{2}\bar{\chi}_c\left(i\not{\partial}_\perp + \not{\mathcal{A}}_{c\perp}\right)\frac{1}{in_+\partial} ix^\mu_\perp\gamma^\nu_\perp\left[\mathcal{B}^+_\nu, \mathcal{B}^+_\mu\right]\frac{\not{n}_+}{2}\chi_c + \text{h.c.},\\
\mathcal{L}^{(1)}_{\xi q} &= \bar{q}_+\not{\mathcal{A}}_{c\perp}\chi_c + \text{h.c.},\\
\mathcal{L}^{(2)}_{\xi q} &= \bar{q}_+\left[in_-\partial + n_-\mathcal{A}_c + \left(i\not{\partial}_\perp + \not{\mathcal{A}}_c\right)\frac{1}{in_+\partial}\left(i\not{\partial}_\perp + \not{\mathcal{A}}_c\right)\right]\frac{\not{n}_+}{2}\chi_c\\
&\quad + \bar{q}_+\left(i\overleftarrow{\partial}^\mu + \mathcal{B}^\mu_+\right)x_{\perp\mu}\left(i\not{\partial}_\perp + \not{\mathcal{A}}_c\right)\chi_c + \text{h.c.}\,.
\end{aligned}
\tag{A.1}
$$

A.2 YM subleading SCET Lagrangian

The subleading-power gluon self-interaction terms of the soft-collinear Yang-Mills Lagrangian [29] expressed in terms of the collinear and soft gauge-invariant fields are given by

$$
\begin{aligned}
\mathcal{L}^{(1)}_{1\text{YM}} &= -\frac{1}{g_s^2}\text{tr}\Big(\left[n_+\partial\,\mathcal{A}^c_{\nu_\perp}\right]\left[x^\rho_\perp\, in_-\partial\,\mathcal{B}^+_\rho, \mathcal{A}^{\nu_\perp}_c\right]\Big),\\
\mathcal{L}^{(1)}_{2\text{YM}} &= -\frac{1}{g_s^2}\text{tr}\Big(\left[n_+\partial\,\mathcal{A}^{\nu_\perp}_c\right] in_-\partial\,\mathcal{B}^+_{\nu_\perp}\Big),\\
\mathcal{L}^{(2)}_{1\text{YM}} &= -\frac{1}{2g_s^2}\text{tr}\Big(\left[n_+\partial\,\mathcal{A}^c_{\nu_\perp}\right]\left[n_-x\, in_-\partial\, n_+\mathcal{B}^+,\, \mathcal{A}^{\nu_\perp}_c\right]\Big),\\
\mathcal{L}^{(2)}_{2\text{YM}} &= -\frac{1}{2g_s^2}\text{tr}\Big(\left[n_+\partial\,\mathcal{A}^c_{\nu_\perp}\right]\left[x^\rho_\perp x_{\perp\omega}\left[\partial^\omega,\, in_-\partial\,\mathcal{B}^+_\rho\right],\, \mathcal{A}^{\nu_\perp}_c\right]\Big),\\
\mathcal{L}^{(2)}_{3\text{YM}} &= -\frac{1}{2g_s^2}\text{tr}\Big(\left[n_+\partial\,\mathcal{A}^c_{\nu_\perp}\right]\left[x^\rho_\perp x_{\perp\omega}\left[\mathcal{B}^\omega_+, n_-\partial\,\mathcal{B}^+_\rho\right],\, \mathcal{A}^{\nu_\perp}_c\right]\Big),\\
\mathcal{L}^{(2)}_{4\text{YM}} &= -\frac{1}{2g_s^2}\text{tr}\Big(\left[n_+\partial\,\mathcal{A}^c_{\nu_\perp}\right]\left[x^\rho_\perp\left[i\partial_\rho\mathcal{B}^+_{\nu_\perp} - i\partial_{\nu_\perp}\mathcal{B}^+_\rho\right],\, n_-\mathcal{A}_c\right]\Big),\\
\mathcal{L}^{(2)}_{5\text{YM}} &= -\frac{1}{2g_s^2}\text{tr}\Big(\left[n_+\partial\,\mathcal{A}^c_{\nu_\perp}\right]\left[x^\rho_\perp\left[\mathcal{B}^+_\rho, \mathcal{B}^+_{\nu_\perp}\right],\, n_-\mathcal{A}_c\right]\Big),\\
\mathcal{L}^{(2)}_{6\text{YM}} &= -\frac{1}{g_s^2}\text{tr}\Big(\left[i\partial^{\mu_\perp}\mathcal{A}^{\nu_\perp}_c - i\partial^{\nu_\perp}\mathcal{A}^{\mu_\perp}_c\right]\left[ix^\rho_\perp\left[i\partial_\rho\mathcal{B}^+_{\mu_\perp} - i\partial_{\mu_\perp}\mathcal{B}^+_\rho\right],\, \mathcal{A}^c_{\nu_\perp}\right]\Big),\\
\mathcal{L}^{(2)}_{7\text{YM}} &= -\frac{1}{g_s^2}\text{tr}\Big(\left[\mathcal{A}^{\mu_\perp}_c, \mathcal{A}^{\nu_\perp}_c\right]\left[ix^\rho_\perp\left[i\partial_\rho\mathcal{B}^+_{\mu_\perp} - i\partial_{\mu_\perp}\mathcal{B}^+_\rho\right],\, \mathcal{A}^c_{\nu_\perp}\right]\Big),\\
\mathcal{L}^{(2)}_{8\text{YM}} &= -\frac{1}{g_s^2}\text{tr}\Big(\left[i\partial^{\mu_\perp}\mathcal{A}^{\nu_\perp}_c - i\partial^{\nu_\perp}\mathcal{A}^{\mu_\perp}_c\right]\left[ix^\rho_\perp\left[\mathcal{B}^+_\rho, \mathcal{B}^+_{\mu_\perp}\right],\, \mathcal{A}^c_{\nu_\perp}\right]\Big),\\
\mathcal{L}^{(2)}_{9\text{YM}} &= -\frac{1}{g_s^2}\text{tr}\Big(\left[\mathcal{A}^{\mu_\perp}_c, \mathcal{A}^{\nu_\perp}_c\right]\left[ix^\rho_\perp\left[\mathcal{B}^+_\rho, \mathcal{B}^+_{\mu_\perp}\right],\, \mathcal{A}^c_{\nu_\perp}\right]\Big),\\
\mathcal{L}^{(2)}_{10\text{YM}} &= -\frac{1}{2g_s^2}\text{tr}\Big(\left[n_+\partial\, n_-\mathcal{A}^c\right] n_-\partial\, n_+\mathcal{B}^+\Big),\\
\mathcal{L}^{(2)}_{11\text{YM}} &= \frac{1}{g_s^2}\text{tr}\Big(\left(i\partial^{\mu_\perp}\mathcal{A}^{\nu_\perp}_c - i\partial^{\nu_\perp}\mathcal{A}^{\mu_\perp}_c\right)\left(i\partial_{\mu_\perp}\mathcal{B}^+_{\nu_\perp} - i\partial_{\nu_\perp}\mathcal{B}^+_{\mu_\perp}\right)\Big),\\
\mathcal{L}^{(2)}_{12\text{YM}} &= \frac{1}{g_s^2}\text{tr}\Big(\left[\mathcal{A}^{\mu_\perp}_c, \mathcal{A}^{\nu_\perp}_c\right]\left(i\partial_{\mu_\perp}\mathcal{B}^+_{\nu_\perp} - i\partial_{\nu_\perp}\mathcal{B}^+_{\mu_\perp}\right)\Big),
\end{aligned}
$$

JHEP07(2020)078

$$
\begin{aligned}
\mathcal{L}^{(2)}_{13\mathrm{YM}} &= \frac{1}{g_s^2}\mathrm{tr}\Big(\big(i\partial^{\mu_\perp}\mathcal{A}_c^{\nu_\perp} - i\partial^{\nu_\perp}\mathcal{A}_c^{\mu_\perp}\big)\,\big[\mathcal{B}^+_{\mu_\perp},\mathcal{B}^+_{\nu_\perp}\big]\Big),\\
\mathcal{L}^{(2)}_{14\mathrm{YM}} &= \frac{1}{g_s^2}\mathrm{tr}\Big(\big[\mathcal{A}_c^{\mu_\perp},\mathcal{A}_c^{\nu_\perp}\big]\,\big[\mathcal{B}^+_{\mu_\perp},\mathcal{B}^+_{\nu_\perp}\big]\Big),\\
\mathcal{L}^{(2)}_{15\mathrm{YM}} &= -\frac{1}{g_s^2}\mathrm{tr}\Big(\big[n_+\partial\,\mathcal{A}_c^{\nu_\perp}\big]x_{\perp\sigma}\big[\partial^\sigma, n_-\partial B^+_{\nu_\perp}\big]\Big),\\
\mathcal{L}^{(2)}_{16\mathrm{YM}} &= \frac{1}{g_s^2}\mathrm{tr}\Big(\big[n_+\partial\,\mathcal{A}_c^{\nu_\perp}\big]x_{\perp\sigma}\big[iB^\sigma_+, n_-\partial B^+_{\nu_\perp}\big]\Big).
\end{aligned}
\tag{A.2}
$$

B One-loop single soft real emission amplitude

In the main body of the text we focused on the factorization formula at the cross-section level. As a by-product of the computation of the collinear functions, which are amplitude-level objects, we also obtained the power-suppressed one-loop one-soft emission DY amplitude, which we summarize here. The results below, computed directly in SCET, were shown to agree with in-house results obtained by applying the expansion-by-regions method to the same quantity.

We consider the following operator, which is the right-hand side of (3.4) without the soft current J_s:

$$
\sum_{m_1,m_2}\int \{dt_k\}\,\{d\bar{t}_{\bar{k}}\}\,\widetilde{C}^{\,m_1,m_2}\left(\{t_k\},\{\bar{t}_{\bar{k}}\}\right)J_\rho^{m_1,m_2}\left(\{t_k\},\{\bar{t}_{\bar{k}}\}\right) \tag{B.1}
$$

where

$$
J_\rho^{m_1,m_2}\left(\{t_k\},\{\bar{t}_{\bar{k}}\}\right) = J_{\bar{c}}^{m_1}(\{\bar{t}_{\bar{k}}\})\,\Gamma_\rho^{m_1,m_2}\,J_c^{m_2}\left(\{t_k\}\right) \tag{B.2}
$$

as in (3.5). The variables appearing in this expression are defined in section 3.1, and the sum is performed over the different power-suppressed currents in the N-jet SCET operator matched to the QCD current.

Below we focus solely on the case in which the power suppression is in the collinear sector, thereby setting $m_1 = A0$, and allow for structures which give power-suppression up to $\mathcal{O}(\lambda^2)$ (NLP). Specifically, we consider the time-ordered product of $J_\rho^{m_1,m_2}$ with subleading-power Lagrangian insertions between an emitted soft gluon $\langle g(k)^K|$, and an incoming collinear quark and anticollinear antiquark, $|q(p)\,\bar{q}(l)\,\rangle$. This defines the amplitude

$$
\mathcal{M}_\rho^K = \langle g(k)^K|\sum_m\int\{dt_k\}\,d\bar{t}\,\widetilde{C}^{A0,m}\left(\{t_k\},\bar{t}\,\right)\,J_\rho^{A0,m}\left(\{t_k\},\bar{t}\,\right)|q(p)\,\bar{q}(l)\rangle\,, \tag{B.3}
$$

that we calculate at the one-loop order. Concretely, we consider only the time-ordered products of the collinear operator part $J_c^{m_2}$ in (B.2) with subleading-power soft-collinear (not: soft-anticollinear) Lagrangian insertions. The complete result for the amplitude is obtained by subtracting from the contributions given below the corresponding ones with n_+ and n_- interchanged.

In the following sections we present the different contributions to this object. Partial results obtained when the virtual loop is collinear (soft) carry a subscript c (s), $\mathcal{M}_c$ ($\mathcal{M}_s$).

JHEP07(2020)078

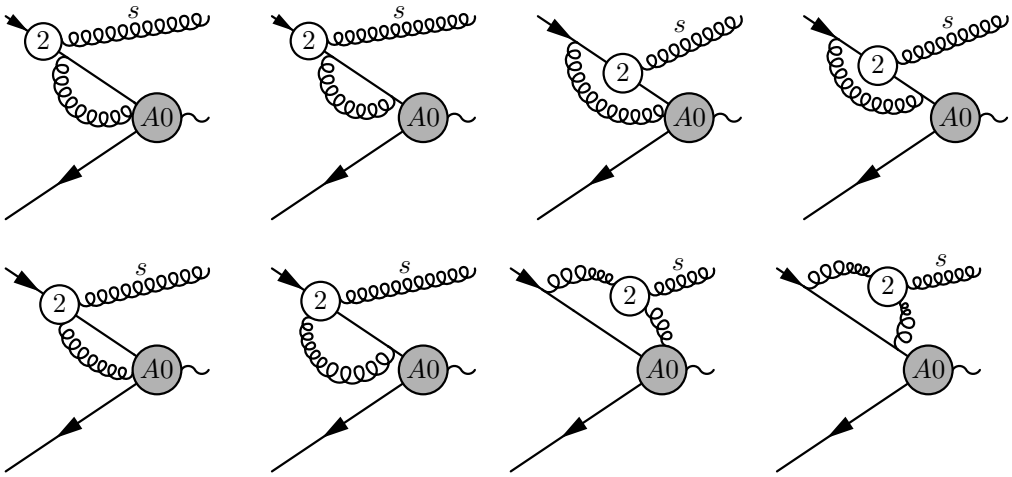

Figure 8. One-loop collinear diagrams with one soft gluon emission. Only the LP current, $A0$, is used here. Power suppression is provided by the time-ordered product insertion of $\mathcal{L}^{(2)}$ Lagrangian terms. The collinear gluon in the loop attaches either to the collinear quark or the collinear Wilson line of the χ_c field, which is part of the $A0$ current. Note the difference in the drawing of the diagrams in those in figure 6: here we included the anticollinear leg and hard current.

The NLO contributions from the one-loop hard matching coefficient are marked with h, $\mathcal{M}_h$. Moreover, we further split the results according to the polarization of the off-shell DY photon γ^* produced by the vector current, that is, we separate the amplitude into the terms proportional to $\gamma_{\perp\rho}$, $n_{+\rho}$, and $n_{-\rho}$. Notice that the $\gamma_{\perp\rho}$ structure appears due to the LP current in (3.2), while $n_{\pm\rho}$ terms arise from the power-suppressed $A1$ and $B1$ currents in (3.18) and (3.19), respectively.

B.1 Collinear loop: $\gamma_{\perp\rho}$

We begin with the results for the set of diagrams in which the virtual loop has collinear momentum scaling and the virtual photon created by the vector current has a transverse ρ index. In (B.3) this means taking the LP current, and index m spans over time-ordered product insertions of the $\mathcal{L}^{(2)}$ Lagrangian. The equations below are in fact related to the results presented in (4.29) and come from calculation of the diagrams in figure 8.

We separate the resulting expression into the amplitude with colour factor C_F and C_A. The former receives contributions from the diagrams in the top line of figure 8, the latter from those in the bottom line and the non-abelian part of the last two diagrams in the top line. We find

$$\begin{aligned}\mathcal{M}^{\gamma_\perp\rho\,K}_{c,C_F} = \bar{v}_{\bar{c}}(l)\gamma^\rho_\perp \frac{ig_s\alpha_s}{(4\pi)}\left[\frac{(n_+p)(n_-k)}{\mu^2}\right]^{-\epsilon}\frac{C_F\mathbf{T}^K}{(n_+p)(n_-k)}\frac{e^{\epsilon\gamma_E}\Gamma[1+\epsilon]\Gamma[1-\epsilon]^2}{(1+\epsilon)(1-\epsilon)\Gamma[2-2\epsilon]} \\ \times\left\{(n_+k)n_{-\nu}\left(\frac{3}{\epsilon}-4-7\epsilon\right)+[\not{k}_\perp,\gamma_{\perp\nu}]\,\frac{1}{2}\left(1-\epsilon^2\right)\right. \\ \left.+k_{\perp\nu}\left(\frac{2}{\epsilon}-5-6\epsilon+\epsilon^2\right)+(n_-k)n_{+\nu}\left(-\frac{1}{\epsilon}-1+\epsilon+\epsilon^2\right)\right\}u_c(p)\epsilon^{*\nu}(k)\,,\end{aligned} \tag{B.4}$$

JHEP07(2020)078

$$\mathcal{M}^{\gamma_\perp\rho\,K}_{c,C_A} = \bar{v}_{\bar{c}}(l)\gamma^\rho_\perp \frac{ig_s\alpha_s}{(4\pi)}\left[\frac{(n_+p)(n_-k)}{\mu^2}\right]^{-\epsilon}\frac{C_A\mathbf{T}^K}{(n_+p)(n_-k)}\frac{e^{\epsilon\gamma_E}\Gamma[1+\epsilon]\Gamma[1-\epsilon]^2}{(1+\epsilon)(1-\epsilon)\Gamma[2-2\epsilon]}$$
$$\times\Big\{(n_+k)n_{-\nu}\frac{1}{2}\Big(-\frac{1}{\epsilon^2}-\frac{1}{\epsilon}-2+11\epsilon+\epsilon^2\Big)+[\not{k}_\perp,\gamma_{\perp\nu}]\frac{1}{2}\left(-1+\epsilon^2\right)$$
$$+k_{\perp\nu}\Big(-\frac{1}{\epsilon^2}-\frac{1}{\epsilon}+3+3\epsilon\Big)+(n_-k)n_{+\nu}\frac{1}{2}\Big(-\frac{1}{\epsilon^2}-\frac{1}{\epsilon}+8-5\epsilon-\epsilon^2\Big)\Big\}u_c(p)\epsilon^{*\nu}(k)\,. \tag{B.5}$$

In this appendix, we use the on-shell condition $k^2=0$ to rewrite $k_\perp^2=-(n_-k)(n_+k)$, but we do not impose the transversality relation (4.13). Notice that in (B.5) there are still $1/\epsilon^2$ poles. These only cancel once soft structures are combined as described in the main text.

B.2 Collinear loop: n_-^ρ and n_+^ρ

These contributions are due to time-ordered products of the power-suppressed hard currents defined in (3.18) and (3.19) with $\mathcal{L}^{(1)}$ Lagrangian insertions. The corresponding diagrams are shown in figure 9. Separating the two colour structures, we find

$$\mathcal{M}^{n_\pm\rho\,K}_{c,C_F} = \bar{v}_{\bar{c}}(l)\left(\frac{n_-^\rho}{n_-l}-\frac{n_+^\rho}{n_+p}\right)\frac{ig_s\alpha_s}{(4\pi)}\left[\frac{(n_+p)(n_-k)}{\mu^2}\right]^{-\epsilon}C_F\mathbf{T}^K\frac{e^{\epsilon\gamma_E}\Gamma[1+\epsilon]\Gamma[1-\epsilon]^2}{(1+\epsilon)(1-\epsilon)\Gamma[2-2\epsilon]}$$
$$\times\left(\gamma_{\perp\nu}-\frac{\not{k}_\perp n_{-\nu}}{(n_-k)}\right)\left(1+2\epsilon+\epsilon^2\right)u_c(p)\epsilon^{*\nu}(k)\,, \tag{B.6}$$

$$\mathcal{M}^{n_\pm\rho\,K}_{c,C_A} = \bar{v}_{\bar{c}}(l)\left(\frac{n_-^\rho}{n_-l}-\frac{n_+^\rho}{n_+p}\right)\frac{ig_s\alpha_s}{(4\pi)}\left[\frac{(n_+p)(n_-k)}{\mu^2}\right]^{-\epsilon}C_A\mathbf{T}^K\frac{e^{\epsilon\gamma_E}\Gamma[1+\epsilon]\Gamma[1-\epsilon]^2}{(1+\epsilon)(1-\epsilon)\Gamma[2-2\epsilon]}$$
$$\times\left(\gamma_{\perp\nu}-\frac{\not{k}_\perp n_{-\nu}}{(n_-k)}\right)\left(\frac{1}{\epsilon}-2\,\epsilon-\epsilon^2\right)u_c(p)\epsilon^{*\nu}(k)\,. \tag{B.7}$$

B.3 Soft loop: $\gamma_{\perp\rho}$

In this section we present the result for the soft one-virtual, one-real soft gluon amplitude proportional to $\gamma_{\perp\rho}$. Only one SCET diagram, shown in figure 10, is needed to reproduce the corresponding virtual-real contribution from the expansion-by-regions method. Hence only non-abelian contributions arise here and we find

$$\mathcal{M}^{\gamma_\perp\rho\,K}_{s,C_A} = \bar{v}_{\bar{c}}(l)\,\gamma^\rho_\perp\frac{ig_s\alpha_s}{(4\pi)}\left(\frac{-(n_-k)(n_+k)}{\mu^2}\right)^{-\epsilon}\frac{C_A\mathbf{T}^K}{(n_+p)(n_-k)}\frac{e^{\epsilon\gamma_E}\Gamma[1+\epsilon]^2\Gamma[1-\epsilon]^3}{\Gamma[2-2\epsilon]}$$
$$\times\Big(n_+k\,n_{-\nu}+k_{\perp\nu}+\frac{1}{2}[\not{k}_\perp,\gamma_{\perp\nu}]\Big)\left(\frac{1}{\epsilon^2}-\frac{2}{\epsilon}\right)u_c(p)\epsilon^{*\nu}(k)\,. \tag{B.8}$$

Details on the vanishing of numerous other a priori possible diagrams are provided in figures 11 and 12. Note that the latter figure also includes diagrams that represent insertions of both, the collinear (on the upper leg) and anticollinear (on the lower leg) subleading soft-collinear interactions, when $a=b=1$. However, as all these terms vanish, there is a unique separation of contributions from collinear Lagrangian insertions and from anticollinear Lagrangian insertions. In (B.8) have we have given the $a=2$, $b=0$ contribution from the last diagram in figure 12, while the $a=0, b=2$ anticollinear one

JHEP07(2020)078

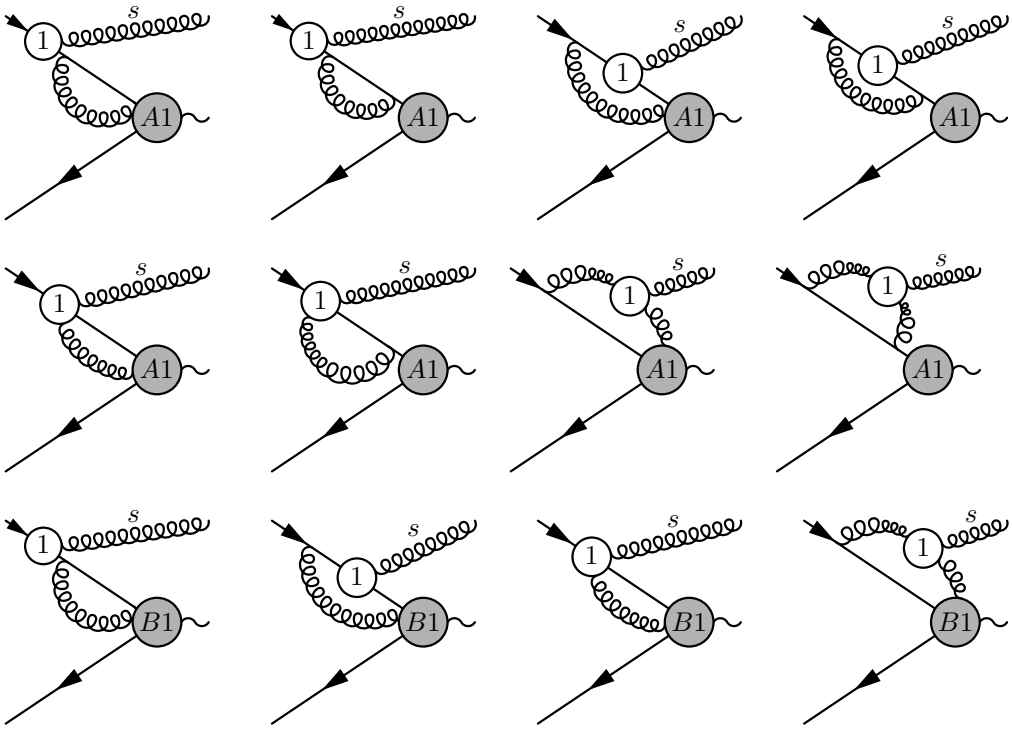

Figure 9. Collinear one-loop diagrams with one soft gluon emission. The $\mathcal{O}(\lambda^1)$ power-suppressed currents $A1$ and $B1$ defined in (3.18) and (3.19), respectively, are used here. The collinear virtual gluon must attach to the $B1$ current, because of the additional $\mathcal{A}_{c\perp}$ gluon field present in this subleading current.

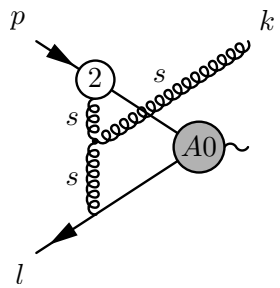

Figure 10. The only diagram relevant to the one virtual, one-real contribution to the two-loop soft function. Here the power suppression is placed on the collinear leg as indicated by the $\mathcal{O}(\lambda^2)$ vertex.

is obtained by exchanging $n_+ \leftrightarrow n_-$. We further note that the absence of a contribution of the second diagram in figure 12, containing a power-suppressed two-soft gluon vertex, implies the statement made in section 5.2.3 that only the single soft-gluon structures with their corresponding soft functions S_1, S_6 contribute at NNLO, of which only S_1 is relevant at cross-section level as explained in the main text.

JHEP07(2020)078

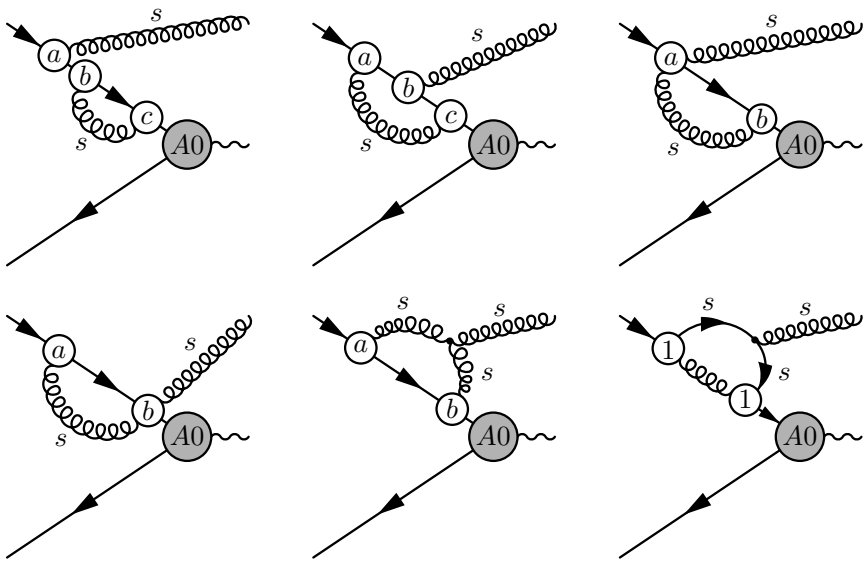

Figure 11. Diagrams with one soft emitted gluon and one soft loop. Since all the diagrams here include the LP $J^{A0,A0}$ current, the $\mathcal{O}(\lambda^2)$ power suppression must be provided by Lagrangian insertions. This means using all possible insertions such that $a + b\,(+c) = 2$ at the indicated vertices. Out of the 20 possibilities, many vanish immediately due to contractions which yield $n_\pm^2 = n_\pm \cdot \gamma_\perp = 0$ or propagators which give zero due to the vanishing external transverse momentum. The remaining integrals, where the integrand does not immediately vanish, are either scaleless or vanish by Cauchy's theorem, because all propagator poles lie in one half of the complex momentum plane.

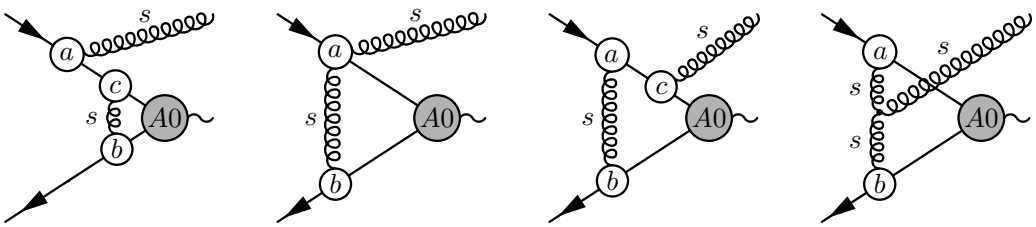

Figure 12. Soft one-loop diagrams with one emitted soft gluon. As in the previous figure, only the LP current is present in these diagrams, however now the virtual soft gluon connects the collinear and anticollinear legs. Lagrangian insertions must again be chosen such that $a + b\,(+c) = 2$. Note that all diagrams with $b = 1$ vanish, since a single leg cannot carry a $\mathcal{O}(\lambda)$ suppression as explained in section 3.2. Only the last diagram with $a = 2$ or $b = 2$ gives a non-vanishing result. The others are either scaleless or vanish after momentum conservation is imposed.

B.4 Soft loop: n_+^ρ

The relevant diagram is again the topology of figure 10. However, since one power of λ is used up by the power-suppressed current, at the soft-collinear vertex we now insert the $\mathcal{L}^{(1)}$ term from the SCET Lagrangian.

The $J^{A0,B1}$ current cannot give a contribution here since it produces a collinear gluon, that cannot be contracted to form a soft loop.

JHEP07(2020)078

The diagrams shown in figures 11 and 12 are also present here. The only change is that the LP hard current is replaced by $J^{A0,A1}$ and the sum of $a+b\,(+c)=1$ only. Once again only the last diagram in figure 12 does not vanish, and we find

$$\mathcal{M}^{n_+\rho\,K}_{s,C_A} = \bar{v}_{\bar{c}}(l)\, n_+^\rho \frac{ig_s\alpha_s}{(4\pi)} \left(\frac{-(n_-k)(n_+k)}{\mu^2}\right)^{-\epsilon} \frac{C_A\mathbf{T}^K}{(n_+p)} \frac{e^{\epsilon\gamma_E}\Gamma[1+\epsilon]^2\,\Gamma[1-\epsilon]^3}{\Gamma[2-2\epsilon]} \times \left[\gamma_{\perp\nu}\frac{1}{\epsilon^2} + \frac{k_{\perp\nu}\not{k}_\perp}{(n_-k)(n_+k)}\frac{1}{\epsilon^2} + \left(\frac{n_{+\nu}}{(n_+k)} - \frac{n_{-\nu}}{(n_-k)}\right)\not{k}_\perp\left(\frac{1}{2\epsilon^2}-\frac{1}{\epsilon}\right)\right] u_c(p)\epsilon^{*\nu}(k)\,. \tag{B.9}$$

There is no term proportional to n_-^ρ.

B.5 Hard loop: $\gamma_{\perp\rho}$

As discussed in the main text, there exists also a contribution to the NLO NLP amplitude from the one-loop hard matching coefficient $C^{\,A0,A0}$ given in (5.5). We obtain

$$\begin{aligned}\mathcal{M}^{\gamma_\perp\rho\,K}_{h,C_F} &= \bar{v}_{\bar{c}}(l)\,\gamma_\perp^\rho \frac{ig_s\alpha_s}{(4\pi)}\left(\frac{-(n_-l)(n_+p)}{\mu^2}\right)^{-\epsilon}\frac{C_F\mathbf{T}^K}{(n_+p)(n_-k)} \\ &\times\Bigg((n_+k)n_{-\nu}\left(\frac{2}{\epsilon^2}+\frac{1}{\epsilon}+5-\frac{\pi^2}{6}\right) + [\not{k}_\perp,\gamma_{\perp\nu}]\left(\frac{1}{\epsilon^2}+\frac{3}{2\epsilon}-\frac{\pi^2}{12}+4\right) \\ &+ k_{\perp\nu}\left(\frac{2}{\epsilon^2}+\frac{3}{\epsilon}-\frac{\pi^2}{6}+8\right) + (n_-k)n_{+\nu}\left(\frac{2}{\epsilon}+3\right) + \mathcal{O}(\epsilon)\Bigg)\, u_c(p)\epsilon^{*\nu}(k)\,,\end{aligned} \tag{B.10}$$

and $\mathcal{M}^{\gamma_\perp\rho\,K}_{h,C_A} = 0$.

B.6 Hard loop: n_+^ρ

This contribution comes from the one-loop correction to the matching coefficient $C^{\,A0,A1}$ of the $J^{A0,A1}$ current together with an insertion of the $\mathcal{O}(\lambda)$ piece of quark SCET Lagrangian. $C^{\,A0,A1}$ is related to $C^{\,A0,A0}$ by reparametrization invariance [46]. With the definition (3.18) the relation reads $C^{\,A0,A1} = -1/(n_+p)\,C^{\,A0,A0}$. We then find

$$\begin{aligned}\mathcal{M}^{n_+\rho\,K}_{h,C_F} &= \bar{v}_{\bar{c}}(l)\,n_+^\rho\frac{ig_s\alpha_s}{4\pi}\left(\frac{-(n_-l)(n_+p)}{\mu^2}\right)^{-\epsilon}\frac{C_F\mathbf{T}^K}{(n_+p)(n_-k)}\left(\not{k}_\perp n_{-\nu} - (n_-k)\gamma_{\perp\nu}\right) \\ &\times\left(-\frac{2}{\epsilon^2}-\frac{3}{\epsilon}-8+\frac{\pi^2}{6}+\mathcal{O}(\epsilon)\right) u_c(p)\epsilon^{*\nu}(k)\,.\end{aligned} \tag{B.11}$$

There is no term proportional to n_-^ρ.

Open Access. This article is distributed under the terms of the Creative Commons Attribution License (CC-BY 4.0), which permits any use, distribution and reproduction in any medium, provided the original author(s) and source are credited.

JHEP07(2020)078

References

[1] G.F. Sterman, *Summation of Large Corrections to Short Distance Hadronic Cross-Sections*, *Nucl. Phys. B* **281** (1987) 310 [INSPIRE].

[2] S. Catani and L. Trentadue, *Resummation of the QCD Perturbative Series for Hard Processes*, *Nucl. Phys. B* **327** (1989) 323 [INSPIRE].

[3] A. Idilbi and X.-d. Ji, *Threshold resummation for Drell-Yan process in soft-collinear effective theory*, *Phys. Rev. D* **72** (2005) 054016 [hep-ph/0501006] [INSPIRE].

[4] A. Idilbi, X.-d. Ji and F. Yuan, *Resummation of threshold logarithms in effective field theory for DIS, Drell-Yan and Higgs production*, *Nucl. Phys. B* **753** (2006) 42 [hep-ph/0605068] [INSPIRE].

[5] T. Becher, M. Neubert and G. Xu, *Dynamical Threshold Enhancement and Resummation in Drell-Yan Production*, *JHEP* **07** (2008) 030 [arXiv:0710.0680] [INSPIRE].

[6] S. Moch and A. Vogt, *Higher-order soft corrections to lepton pair and Higgs boson production*, *Phys. Lett. B* **631** (2005) 48 [hep-ph/0508265] [INSPIRE].

[7] D. Bonocore, E. Laenen, L. Magnea, L. Vernazza and C.D. White, *The method of regions and next-to-soft corrections in Drell-Yan production*, *Phys. Lett. B* **742** (2015) 375 [arXiv:1410.6406] [INSPIRE].

[8] N. Bahjat-Abbas, J. Sinninghe Damsté, L. Vernazza and C.D. White, *On next-to-leading power threshold corrections in Drell-Yan production at N^3LO*, *JHEP* **10** (2018) 144 [arXiv:1807.09246] [INSPIRE].

[9] E. Laenen, L. Magnea and G. Stavenga, *On next-to-eikonal corrections to threshold resummation for the Drell-Yan and DIS cross sections*, *Phys. Lett. B* **669** (2008) 173 [arXiv:0807.4412] [INSPIRE].

[10] E. Laenen, G. Stavenga and C.D. White, *Path integral approach to eikonal and next-to-eikonal exponentiation*, *JHEP* **03** (2009) 054 [arXiv:0811.2067] [INSPIRE].

[11] E. Laenen, L. Magnea, G. Stavenga and C.D. White, *Next-to-Eikonal Corrections to Soft Gluon Radiation: A Diagrammatic Approach*, *JHEP* **01** (2011) 141 [arXiv:1010.1860] [INSPIRE].

[12] D. Bonocore, E. Laenen, L. Magnea, S. Melville, L. Vernazza and C.D. White, *A factorization approach to next-to-leading-power threshold logarithms*, *JHEP* **06** (2015) 008 [arXiv:1503.05156] [INSPIRE].

[13] D. Bonocore, E. Laenen, L. Magnea, L. Vernazza and C.D. White, *Non-abelian factorisation for next-to-leading-power threshold logarithms*, *JHEP* **12** (2016) 121 [arXiv:1610.06842] [INSPIRE].

[14] M. Beneke et al., *Leading-logarithmic threshold resummation of the Drell-Yan process at next-to-leading power*, *JHEP* **03** (2019) 043 [arXiv:1809.10631] [INSPIRE].

[15] M. Beneke, M. Garny, S. Jaskiewicz, R. Szafron, L. Vernazza and J. Wang, *Leading-logarithmic threshold resummation of Higgs production in gluon fusion at next-to-leading power*, *JHEP* **01** (2020) 094 [arXiv:1910.12685] [INSPIRE].

[16] N. Bahjat-Abbas et al., *Diagrammatic resummation of leading-logarithmic threshold effects at next-to-leading power*, *JHEP* **11** (2019) 002 [arXiv:1905.13710] [INSPIRE].

JHEP07(2020)078

[17] R. Boughezal, X. Liu and F. Petriello, *Power Corrections in the N-jettiness Subtraction Scheme*, *JHEP* **03** (2017) 160 [arXiv:1612.02911] [INSPIRE].

[18] I. Moult, L. Rothen, I.W. Stewart, F.J. Tackmann and H.X. Zhu, *Subleading Power Corrections for N-Jettiness Subtractions*, *Phys. Rev. D* **95** (2017) 074023 [arXiv:1612.00450] [INSPIRE].

[19] I. Moult, L. Rothen, I.W. Stewart, F.J. Tackmann and H.X. Zhu, *N-jettiness subtractions for $gg \to H$ at subleading power*, *Phys. Rev. D* **97** (2018) 014013 [arXiv:1710.03227] [INSPIRE].

[20] M.A. Ebert, I. Moult, I.W. Stewart, F.J. Tackmann, G. Vita and H.X. Zhu, *Power Corrections for N-Jettiness Subtractions at $\mathcal{O}(\alpha_s)$*, *JHEP* **12** (2018) 084 [arXiv:1807.10764] [INSPIRE].

[21] R. Boughezal, A. Isgrò and F. Petriello, *Next-to-leading-logarithmic power corrections for N-jettiness subtraction in color-singlet production*, *Phys. Rev. D* **97** (2018) 076006 [arXiv:1802.00456] [INSPIRE].

[22] R. Boughezal, A. Isgrò and F. Petriello, *Next-to-leading power corrections to $V+1$ jet production in N-jettiness subtraction*, *Phys. Rev. D* **101** (2020) 016005 [arXiv:1907.12213] [INSPIRE].

[23] M.A. Ebert, I. Moult, I.W. Stewart, F.J. Tackmann, G. Vita and H.X. Zhu, *Subleading power rapidity divergences and power corrections for q_T*, *JHEP* **04** (2019) 123 [arXiv:1812.08189] [INSPIRE].

[24] L. Cieri, C. Oleari and M. Rocco, *Higher-order power corrections in a transverse-momentum cut for colour-singlet production at NLO*, *Eur. Phys. J. C* **79** (2019) 852 [arXiv:1906.09044] [INSPIRE].

[25] I. Moult, I.W. Stewart, G. Vita and H.X. Zhu, *First Subleading Power Resummation for Event Shapes*, *JHEP* **08** (2018) 013 [arXiv:1804.04665] [INSPIRE].

[26] V. Del Duca, *High-energy Bremsstrahlung Theorems for Soft Photons*, *Nucl. Phys. B* **345** (1990) 369 [INSPIRE].

[27] V. Del Duca, E. Laenen, L. Magnea, L. Vernazza and C.D. White, *Universality of next-to-leading power threshold effects for colourless final states in hadronic collisions*, *JHEP* **11** (2017) 057 [arXiv:1706.04018] [INSPIRE].

[28] M. Beneke, A.P. Chapovsky, M. Diehl and T. Feldmann, *Soft collinear effective theory and heavy to light currents beyond leading power*, *Nucl. Phys. B* **643** (2002) 431 [hep-ph/0206152] [INSPIRE].

[29] M. Beneke and T. Feldmann, *Multipole expanded soft collinear effective theory with nonAbelian gauge symmetry*, *Phys. Lett. B* **553** (2003) 267 [hep-ph/0211358] [INSPIRE].

[30] C.W. Bauer, S. Fleming, D. Pirjol and I.W. Stewart, *An Effective field theory for collinear and soft gluons: Heavy to light decays*, *Phys. Rev. D* **63** (2001) 114020 [hep-ph/0011336] [INSPIRE].

[31] C.W. Bauer, D. Pirjol and I.W. Stewart, *Soft collinear factorization in effective field theory*, *Phys. Rev. D* **65** (2002) 054022 [hep-ph/0109045] [INSPIRE].

[32] G.P. Korchemsky and G. Marchesini, *Resummation of large infrared corrections using Wilson loops*, *Phys. Lett. B* **313** (1993) 433 [INSPIRE].

JHEP07(2020)078

[33] M. Beneke, F. Campanario, T. Mannel and B.D. Pecjak, *Power corrections to $\bar{B} \to X_u \ell \bar{\nu}\,(X_s\gamma)$ decay spectra in the 'shape-function' region*, *JHEP* **06** (2005) 071 [hep-ph/0411395] [INSPIRE].

[34] M. Beneke, M. Garny, R. Szafron and J. Wang, *Anomalous dimension of subleading-power N-jet operators*, *JHEP* **03** (2018) 001 [arXiv:1712.04416] [INSPIRE].

[35] M. Beneke, M. Garny, R. Szafron and J. Wang, *Anomalous dimension of subleading-power N-jet operators. Part II*, *JHEP* **11** (2018) 112 [arXiv:1808.04742] [INSPIRE].

[36] M. Beneke, M. Garny, R. Szafron and J. Wang, *Violation of the Kluberg-Stern-Zuber theorem in SCET*, *JHEP* **09** (2019) 101 [arXiv:1907.05463] [INSPIRE].

[37] T. Matsuura and W.L. van Neerven, *Second Order Logarithmic Corrections to the Drell-Yan Cross-section*, *Z. Phys. C* **38** (1988) 623 [INSPIRE].

[38] S.W. Bosch, M. Neubert and G. Paz, *Subleading shape functions in inclusive B decays*, *JHEP* **11** (2004) 073 [hep-ph/0409115] [INSPIRE].

[39] K.S.M. Lee and I.W. Stewart, *Factorization for power corrections to $B \to X_s\gamma$ and $B \to X_u \ell \bar{\nu}$*, *Nucl. Phys. B* **721** (2005) 325 [hep-ph/0409045] [INSPIRE].

[40] A.J. Larkoski, D. Neill and I.W. Stewart, *Soft Theorems from Effective Field Theory*, *JHEP* **06** (2015) 077 [arXiv:1412.3108] [INSPIRE].

[41] M. Beneke, M. Garny, R. Szafron and J. Wang, *Subleading-power N-jet operators and the LBK amplitude in SCET*, PoS(RADCOR2017)048 [arXiv:1712.07462] [INSPIRE].

[42] R. Hamberg, W.L. van Neerven and T. Matsuura, *A complete calculation of the order α_s^2 correction to the Drell-Yan K factor*, *Nucl. Phys. B* **359** (1991) 343 [*Erratum ibid.* **644** (2002)] [INSPIRE].

[43] M. Beneke and V.A. Smirnov, *Asymptotic expansion of Feynman integrals near threshold*, *Nucl. Phys. B* **522** (1998) 321 [hep-ph/9711391] [INSPIRE].

[44] Y. Li, S. Mantry and F. Petriello, *An Exclusive Soft Function for Drell-Yan at Next-to-Next-to-Leading Order*, *Phys. Rev. D* **84** (2011) 094014 [arXiv:1105.5171] [INSPIRE].

[45] T. Gehrmann, E.W.N. Glover, T. Huber, N. Ikizlerli and C. Studerus, *Calculation of the quark and gluon form factors to three loops in QCD*, *JHEP* **06** (2010) 094 [arXiv:1004.3653] [INSPIRE].

[46] C. Marcantonini and I.W. Stewart, *Reparameterization Invariant Collinear Operators*, *Phys. Rev. D* **79** (2009) 065028 [arXiv:0809.1093] [INSPIRE].

JHEP07(2020)078